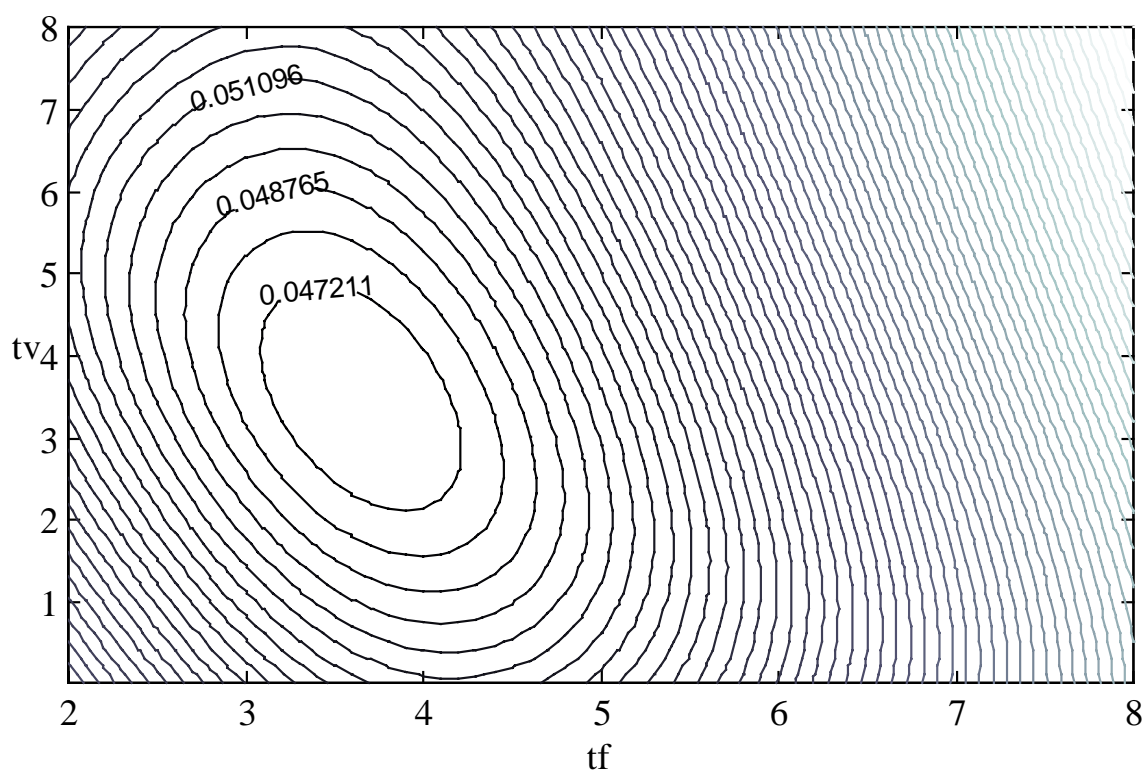


# Optimization of Semi-Empirical Parameters in the FFA-Beddoes Dynamic Stall Model

Murat Mert



 **FLYGTEKNISKA  
FÖRSÖKSANSTALTEN**  
**THE AERONAUTICAL RESEARCH INSTITUTE OF SWEDEN**  
*Box 11021, SE-161 11 Bromma, Sweden*  
*Phone +46 8 555 49 000, Fax +46 8 25 34 81*

## Abstract

Unsteady aerodynamic effects, like dynamic stall, must be considered in calculation of dynamic forces for wind turbines. Models incorporated in aero-elastic programs are of semi-empirical nature. Resulting aerodynamic forces therefore depend on values used for the semi-empirical parameters. In this report a study of finding appropriate parameters to use with the FFA- Beddoes-Leishman dynamic stall model is discussed. Minimization of the deviation between results from 2D wind tunnel tests and simulation with the model is used to find optimum values for the parameters.

The optimization program MMA, Method of Moving Asymptotes is used to optimize parameters in the model for nonlinear aerodynamics.

The optimization program MMA has been modified to work for problems with a quadratic object function without constraints.

The resulting optimum parameters show a large variation from case to case. Using these different sets of optimum parameters in the calculation of blade vibrations give rise to quite different predictions of aerodynamic damping.



# Table of Contents

<b>1</b>	<b>Introduction .....</b>	<b>9</b>
1.1	Background .....	9
<b>2</b>	<b>The Dynamic Stall Model .....</b>	<b>11</b>
2.1	The Phenomenon of Dynamic Stall .....	11
2.2	The FFA Dynamic Stall Model.....	13
<b>3</b>	<b>The Optimization Program.....</b>	<b>17</b>
3.1	The optimization problem .....	17
3.2	Description of MMA, the Method of Moving Asymptotes .....	18
3.3	Modifications of MMA.....	21
3.4	Structure of the optimization program.....	22
3.5	How to use the optimization program.....	23
<b>4</b>	<b>Optimization.....</b>	<b>25</b>
4.1	Cases of optimization and type of objective function.....	25
4.2	Effect of small errors in wind tunnel measurements.....	26
4.3	Optimization Results .....	28
4.3.1	Results from CFD .....	42
4.4	Shortcoming of the dynamic stall model .....	47
4.5	The Root Mean Square function and Comparison between different cases. ....	49
4.6	Tf as a function of the separation point.....	55
<b>5</b>	<b>Conclusions .....</b>	<b>61</b>
	<b>Acnowledgements .....</b>	<b>63</b>
	<b>References .....</b>	<b>65</b>
	<b>Appendix .....</b>	<b>67</b>



## Nomenclature

$a_{cd}$	A constant in the $C_{d,sep}$ equation.
$c$	Chord length, [m]
$C_d$	Drag force coefficient.
$C_l$	Lift force coefficient.
$C_{l\alpha}$	$\frac{\partial C_l}{\partial \alpha}$ , [rad <sup>-1</sup> ].
$C_{lmax}$	Maximum value of $C_l$ .
$C_{l,f}$	The lift force coefficient being a function of the separation point $f$ .
$C_{l,steady}$	Static lift force coefficient.
$C_{l,v}$	The vortex lift force coefficient.
$C_n$	Normal force coefficient.
$C_x$	Tangential force coefficient, positive towards the leading edge, i.e in the opposite x-direction.
$c_v$	Increment in vortex lift.
$f$	Distance from the leading edge to point of separation divided by $c$ . Also interpolating function.
$h$	Distance perpendicular to the chord.
$k$	Reduced frequency, $\frac{\omega \cdot c}{2 \cdot V}$
$s$	Non-dimensional time, $\frac{2 \cdot V \cdot t}{c}$ .
$t$	Time,[s].
$T_f$	Non-dimensional time constant.
$T_p$	Non-dimensional time constant.
$T_v$	Non-dimensional time constant.

$V$	Free stream wind speed, [m/s].
$x$	Chord wise distance from the leading edge, [m].
$\alpha$	Angle of attack, [deg]
$\alpha_0$	Angle of attack at $C_l=0$ .
$\alpha_f$	A substitute value for the effective angle of attack.
$\eta$	Weight coefficient in the objective function.
$\omega$	Rotational frequency, [rad/s].

## Subscripts

$exp$	Data for wind tunnel measurement or Navier-Stokes calculation.
$sim$	Model simulation.
$i$	Component i of a quantity.
$j$	Component j of a quantity.



# 1 Introduction

## 1.1 Background

A majority of today's working wind turbines use stall regulation for passive control of maximum power and loads. Operation with the blades partially in stall is part of their normal operation and the calculation of loads in the stall region is crucial for the design of stall regulated wind turbines.

Engineering models consist of a mixture of physical aspects transformed into equations containing parameters of initially unknown size. It is important for these models to have data from measurements available such that good numerical values can be selected for these parameters. These initially unknown parameters are often referred to as "tuning parameters". The usefulness of the semi-empirical models is, however, dependent on that physical mechanisms of dynamic stall are correctly enough described and that proper values for semi-empirical constants can be found.

In this report the optimization program MMA, is used to optimize some tuning parameters in the FFA-Beddoes-Leishman dynamic stall model.



## 2 The Dynamic Stall Model

### 2.1 The Phenomenon of Dynamic Stall

The term “ dynamic stall ” is most often used to describe the complex series of events that result in dynamic delay of stall to higher angles of attack than the static stall angle. This will e.g. lead to lift coefficients exceeding the static  $C_{l_{\max}}$ . The attendant aerodynamic forces and moments exhibit large amounts of hysteresis with respect to the instantaneous angle of attack.

Even though, in the past, most attention has been given to dynamic stall on helicopter blades, the phenomenon also occurs on jet engine compressor blades, rapidly maneuvering aircraft and wind turbine blades.

Fig 2.1 [1] shows the development of  $C_n$  and  $C_m$  versus angle of attack  $\alpha$  and the corresponding boundary layer behavior for a dynamically stalling airfoil. The information is for a NACA 0012 airfoil oscillated in pitch, but the development of stall is - except for some differences for thick airfoils and small amplitudes - similar in almost all airfoils experiencing fully developed dynamic stall.

Two main characteristics of dynamic stall are the delay in the separation process and the vortex-shedding process. At point (a) in Fig 2.1 there is not any noticeable change in the flow around the pitching airfoil passing the static-stall angle. The first indication of disturbance in the viscous flow is seen to be appearing at point (b), when the flow reverses near the surface at the rear of the airfoil. This reversal progresses up the airfoil surface; then at an angle that depends on many parameters, including airfoil shape, pitch rate, frequency, Reynolds number and Mach number as well as three-dimensional effects, the viscous flow no longer remains thin and attached, and a very strong vortical flow develops. This vortex begins near the leading edge of the airfoil point (e) in Fig 2.1, enlarges, and then moves down the airfoil, inducing strong pitching-moment effects on the airfoil (points (f) and (i)), producing the phenomenon known as dynamic stall. As the angle of attack decreases, the vortex moves into the wake, and a fully separated flow develops on the airfoil. It is worth noting that the angle of attack in Fig 2.1 has reached its minimum before lift is reestablished on the airfoil.

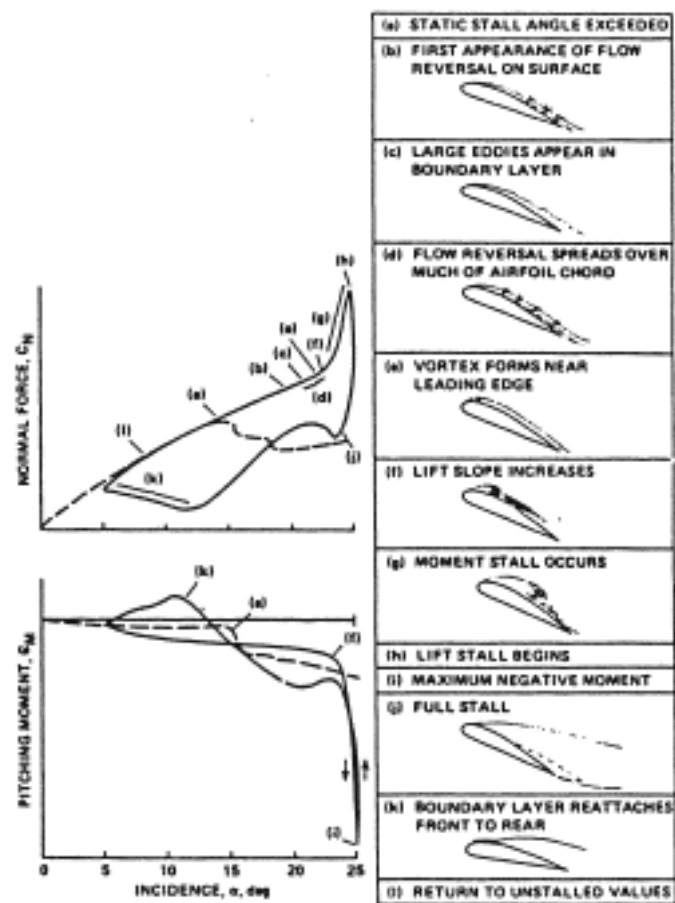


Figure 2.1 Events of dynamic stall on a NACA 0012 airfoil [1].

There are several situations where rapid enough changes of the angle of attack for dynamic stall to be important occur on wind turbine blades. Dynamic stall can be important at angle of attack changes occurring at a rate as low as one per rotor revolution. During nominal field operations, the aerodynamic conditions that produce dynamic stall cannot be prevented. Unsteady turbine inlet velocity profiles are driven naturally by variations in the wind magnitude and direction. Also, inlet flows are altered by obstructions such as tower shadow effects or through flow perturbations introduced by other machines operating upwind on large wind farms.

The resulting transient forces have substantial impacts on operating turbines. Reduced machine life due to fatigue, increased maintenance, and severe transient power spiking are all typical effects. In a rapidly changing unsteady aerodynamic environment unsteady loads can be four to five times larger than predicted steady state values, [2].

Dynamic stall influences the loading of wind turbine rotors in several different ways. Compared to quasi-steady conditions, dynamic “over shoots” in the aerodynamic forces will lead to larger loads. It is also important that for blade oscillations, the phase of the forces will be different from those, which would have been generated by quasi-steady motion. For many cases in stall, the blade oscillations would be unstable if quasi-steady forces would prevail. However, due to the unsteady dynamic stall response, the phase of the aerodynamic forces will be different during an oscillation cycle and the cycle damping can become positive, that is the air extracts energy from the rotor during each cycle of oscillation. It is important to be able to catch this in aeroelastic calculations, through a proper modeling of dynamic stall.

## 2.2 The FFA Dynamic Stall Model

The FFA dynamic stall model is an implementation of the Beddoes-Leishman model, see e.g. [3]. The Beddoes-Leishman model, which is semi-empirical, can shortly be described as an indicial response model for attached flow extended with models for separated flow effects and vortex lift. The model requires only steady two-dimensional data - static  $Cl(\alpha)$  and  $Cd(\alpha)$  - as input for the specific airfoil for which the dynamic forces will be calculated.

The attached flow response to a general angle of attack history is calculated from the superposition of individual indicial responses for each step. This attached flow response is then modified based upon the unsteady separation point. The separation point is given by  $f = x/c$ , where  $x$  is the point of flow separation measured from the leading edge, and  $c$  is the airfoil chord length, see figure 2.2.

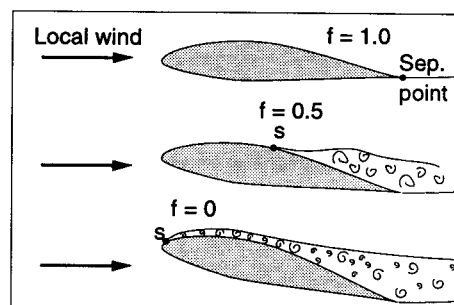


Figure 2.2. Traveling of separation point  $f = x/c$  along the airfoil surface.

One approximation relating the lift force to the separation point is the Kirchoff flow model, given as

$$C_{l,f}(f) = C_{l\alpha} \cdot (\alpha - \alpha_0) \cdot \left( \frac{1 + \sqrt{f}}{2} \right)^2 \quad (2.1)$$

$C_{l\alpha}$  is the lift force curve slope and  $\alpha_0$  is the zero-lift angle of attack.

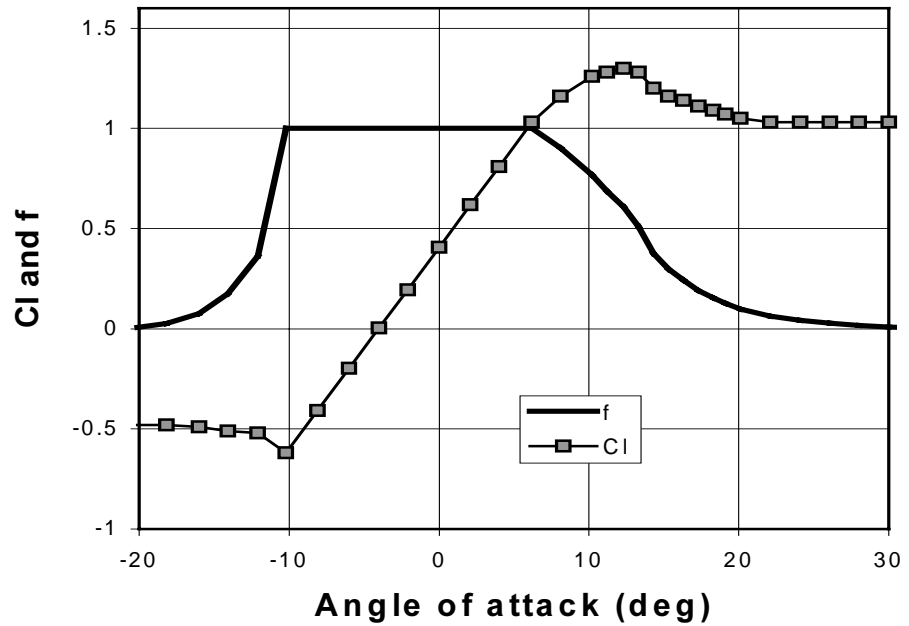


Figure 2.3.  $C_l(\alpha)$  and  $f(\alpha)$  curves.

In figure 2.3 an example of  $f(\alpha)$  and static  $C_l(\alpha)$  curves are seen.  $f(\alpha)$  varies between 1, for fully attached flow, and 0, for totally separated flow, this can also be seen in figure 2.2.

There is a lag in the pressure response along the airfoil for unsteady motion. E.g. the leading edge pressure, which influences the development of the boundary layer and hence the point of separation, will lag its quasi-static value. In the Beddoes-Leishman model this effect is modeled by a shift in angle of attack. The shifted  $\alpha$  represents the quasi-static  $\alpha$  for which the same peak pressure is attained. This  $\alpha$  is used to generate the separation point  $f$ . To obtain the shifted  $\alpha$ , a first order lag, with a time constant  $T_p$ , is applied to  $C_{l,pot}$  in order to produce a substitute value  $C_{l,pot}'$ .

$$\frac{dC'_{l,pot}}{ds} = \frac{C_{l,pot} - C'_{l,pot}}{Tp} \quad (2.2)$$

where  $s$  is the non-dimensional time,  $s = 2 \cdot V \cdot t / c$ .

$C'_{l,pot}$  is then used to define a substitute value for the shifted angle of attack as

$$\alpha_f = \frac{C'_{l,pot}}{C_{l\alpha}} + \alpha_0 \quad (2.3)$$

This  $\alpha_f$  is used to obtain an effective value for the separation point  $f_{static}$ .

$C_{l,pot}$  is derived from unsteady potential flow theory: The indicial method is used to obtain the unsteady circulatory and non- circulatory lift. The circulatory lift is the lift affected by the influence of the shed wake. This is made in the “attached flow” part of the calculation.  $C_{l,pot}$  is a sum of circulatory and non- circulatory lift:

$$C_{l,pot} = C_{l,c} + C_{l,nonc}$$

A great portion of the dynamic effect on lift is obtained by the time lag in the movement of the separation point. The separation points tends to its static value, but lags according to a first order filter with a time constant  **$Tf$** .

$$\frac{df}{ds} = \frac{f_{static} - f}{Tf} \quad (2.4)$$

A vortex lift contribution is also added when the conditions for vortex generation and vortex travel are present. The contribution of vortex lift is a function of the difference between the “attached flow” value of circulatory lift and the lift obtained through the Kirchoff flow model. The vortex lift is computed by assuming that the vortex lift contribution can be viewed as an excess circulation, which is not shed into the wake until some critical condition is reached. Empirically derived time constants are associated with the growth and decay of the vortex lift. The accumulated vortex lift decays exponentially with time but is also updated with new incremental contribution. The time constant for vortex decay,  **$Tv$** , is one of the semi-empirical parameters in the model. The vortex lift is represented by the following equations:

$$c_v = C_{l,c} - C_{l,f} \quad (2.5)$$

$$\frac{dC_{l,v}}{ds} = \frac{\frac{dc_v}{ds} - C_{l,v}}{Tv} \quad (2.6)$$

$C_{l,c}$  is the circulatory lift force coefficient.

In the currently used model, no criterion for the start of ” vortex travelling ” is used, and vortex contribution is allowed as long as the angle of attack is increasing. This fact will give less good simulation results for thin airfoils, were vortex shedding has a great importance.

The vortex lift is assumed to act only in the airfoil normal direction. In order to get zero tangential force contribution a “vortex drag” component is therefore added. The drag is obtained as the static drag plus components of induced drag due to shed wake effects, vortex drag and separation drag,  $C_{d,sep}$

$$C_{d,sep} = a_{cd} (C_{l,static} - C_{l,f}) \quad (2.7)$$

$C_{d,sep}$  is a model of the drag being larger than its static value if the separation point is upstream of its static value and vice versa.

A more detailed description of the FFA-implementation of the Beddoes-Leishman dynamic stall model can be found in [4].



### 3 The Optimization Program

In this chapter the choice of optimization method and structure of the optimization program is described. A description of how to use the program can be found in Appendix 1.

#### 3.1 The optimization problem

To begin, we need an objective function, unknown variables and constraints, if there are any, to define the optimization problem.

##### **Objective function**

In fitting experimental data to a user-defined model, we might minimize the total deviation of observed data from predictions based on the model.

The definition of a relevant objective function is by no means obvious. A good agreement between experiments and simulations could be good agreement in maximum lift. Another objective function that considers the agreement in “mean lift curve slope”, which is very important for aerodynamic damping as pointed out in e.g. [5], is imaginable.

In the current study objective functions based on minimizing the deviation between experiments and simulations have been used.

Objective function 1:

$$f_1 = \sum_{i=1}^k \eta [(C_{l,sim}(t_i) - C_{l,exp}(t_i))^2] \quad (3.1)$$

Objective function 2:

$$f_2 = \sum_{i=1}^k \eta [(C_{n,sim}(t_i) - C_{n,exp}(t_i))^2] + \sum_{i=1}^k (1 - \eta) [(C_{t,sim}(t_i) - C_{t,exp}(t_i))^2] \quad (3.2)$$

##### **Unknown variables**

In fitting-the-data problem, the unknowns are the parameters that define the dynamic stall model.

The resulting lift and drag for unsteady cases will depend on the semi-empirical parameters *Tf*, *Tv*, *acd* and *Tp*.

**Optimization problem**

Find values of the variables that minimize the objective function.

### 3.2 Description of MMA, the Method of Moving Asymptotes

The Method of Moving Asymptotes [9] is a robust optimization program developed by Krister Svanberg at the Royal Institute of Technology in Stockholm. It has been implemented in several large systems for structural optimization, e.g. in OPTSYS at the Aircraft division of Saab-Scania, and in OASIS at ALFGAM Optimization AB.

MMA is an iterative convex approximation method. In each iteration, a convex subproblem, which approximates the original problem, is generated and solved. An important role in the generation of these subproblems is played by a set of parameters which influence the “curvature” of the approximations, and also act as “asymptotes” for the subproblem. By moving these asymptotes, between each iteration, the convergence of the overall process can be stabilized.

The subproblems generated by MMA are then solved by so called dual methods.

Consider an optimization problem of the following general form:

$$\begin{aligned}
 \underline{P}: \quad & \text{minimize} && f_0(\mathbf{x}) && (\mathbf{x} \in \mathcal{R}^n) \\
 & \text{subject to} && f_i(\mathbf{x}) \leq \hat{f}_i && \text{for } i = 1, \dots, m \\
 & \text{and} && x_{j_{\min}} \leq x \leq x_{j_{\max}} && \text{for } j = 1, \dots, n
 \end{aligned}$$

where  $\mathbf{x} = (x_1, \dots, x_n)^T$  is the vector of design variables, in our case  $Tv$ ,  $Tf$ ,  $acd$  and  $TP$ .  $f_0(\mathbf{x})$  is the objective function, the total deviation of observed data from predictions based on the model.  $f_i(\mathbf{x}) \leq \hat{f}_i$  are constraints.  $x_{j_{\min}}$  and  $x_{j_{\max}}$  are the lower and upper bounds on the design variables.

A well-established general approach for attacking such a problem is to generate and solve a sequence of subproblems according to the following iterative scheme:

Step 0. Let index  $k=0$  and choose a starting point  $\mathbf{x}^{(0)}$ .

Step I. Given an iteration point  $\mathbf{x}^{(k)}$ , calculate  $f_i(\mathbf{x}^{(k)})$  and the gradients  $\nabla f_i(\mathbf{x}^{(k)})$  for  $i=0, \dots, m$ .

Step II. Generate a subproblem by replacing the (usually implicit) functions  $f_i$  by approximating explicit functions  $f_i^{(k)}$ , based on the calculations in step I.

Step III. Solve the subproblem and let this optimal solution be the next iteration point  $\mathbf{x}^{(k+1)}$ . Set  $k=k+1$  and go to step I

The process is terminated when some convergence criteria are fulfilled, or simply when the user is satisfied with the current solution  $\mathbf{x}^{(k)}$ .

In MMA, each approximating function  $f_i^{(k)}$  is obtained by a linearization of  $f$  in variables of the type  $1/(U_j - x_j)$  or  $1/(x_j - L_j)$ , where  $L_j$  and  $U_j$  are parameters that satisfy  $L_j < x_j^{(k)} < U_j$  and they are given finite values in each iteration step, which stabilizes the process.  $L_j$  and  $U_j$  are called moving asymptotes.

The approximating functions then looks as follows (for  $i=1, \dots, m$ )

$$f_i^{(k)} = \sum_{j=1}^n \left\{ \frac{p_{ij}}{U_j - x_j} - \frac{q_{ij}}{x_j - L_j} \right\} + r_i \quad (3.3)$$

where  $p_{ij}$ ,  $q_{ij}$  and  $r_i$  are constants based on the calculations in step I and they are updated in every iteration step. This gives the following subproblem:

$$\begin{aligned} \underline{P}^{(k)} : \quad & \text{minimize} && \sum_{j=1}^n \left\{ \frac{p_{0j}}{U_j - x_j} - \frac{q_{0j}}{x_j - L_j} \right\} + r_0 \\ & \text{subject to} && \sum_{j=1}^n \left\{ \frac{p_{ij}}{U_j - x_j} - \frac{q_{ij}}{x_j - L_j} \right\} + r_i \leq \hat{f}_i \quad \text{for } i = 1, \dots, m \\ & \text{and} && \max\{x_{j_{\min}}, \alpha_j\} \leq x_j \leq \min\{x_{j_{\max}}, \beta_j\} \quad \text{for } j = 1, \dots, n \end{aligned}$$

The parameters  $\alpha_j$  and  $\beta_j$  are “move limits” and should be chosen such that

$$L_j \leq \alpha_j \leq x_j \leq \beta_j \leq U_j \quad (3.4)$$

Equation (3.3) is written shortly as  $\mathbf{x} \in \mathbf{X}$ .

The subproblem above is a convex optimization problem, which means that any local optimum to the subproblem is also a global optimum.

A nice property of the convex subproblem is that it can be transformed to an equivalent problem, called the “ dual ” problem.

The Lagrange function corresponding to  $P^{(k)}$  is given by:

$$L(\mathbf{x}, \mathbf{y}) = -\sum_{i=1}^m y_i \left( \hat{f}_i - r_i \right) + \sum_{j=1}^n \left\{ \frac{p_j(\mathbf{y})}{U_j - x_j} - \frac{q_j(\mathbf{y})}{x_j - L_j} \right\} \quad (3.5)$$

Where  $\mathbf{y} = (y_1, \dots, y_m)^T$  is the vector of Lagrange multipliers, which are all required to be non-negative, i.e.  $\mathbf{y} \geq 0$ .

$$p_j(\mathbf{y}) = p_{0j} + \sum_{i=1}^m y_i p_{ij} \quad (3.6)$$

and

$$q_j(\mathbf{y}) = q_{0j} + \sum_{i=1}^m y_i q_{ij} \quad (3.7)$$

For each given  $\mathbf{y} \geq 0$ ,  $L(\mathbf{x}, \mathbf{y})$  is a strict convex function in  $\mathbf{x}$  (over  $\mathbf{X}$ ).

Therefore, there is a unique  $\mathbf{x} = \mathbf{x}(\mathbf{y})$ , which minimizes  $L(\mathbf{x}, \mathbf{y})$  over  $\mathbf{X}$  (for the given  $\mathbf{y} \geq 0$ ). The minimizing  $\mathbf{x} = \mathbf{x}(\mathbf{y})$  can be solved analytically.

The dual objective function is defined as:

$$\phi(\mathbf{y}) = \min\{L(\mathbf{x}, \mathbf{y}) | \mathbf{x} \in \mathbf{X}\} = L(\mathbf{x}(\mathbf{y}), \mathbf{y}) \quad (3.8)$$

The dual problem corresponding to  $P^{(k)}$  is defined as:

$$\begin{array}{lll} \underline{D}: & \text{maximize} & \varphi(\mathbf{y}) \\ & \text{subject to} & \mathbf{y} \leq \mathbf{0} \end{array}$$

with  $\varphi(\mathbf{y})$  as above.

The dual problem is solved with some standard numerical method like a conjugate gradient method or by a Newton method.

Because of the convexity of the constraint functions in  $P^{(k)}$ , and the strict convexity of the objective function the following important fact can be proved:

*If  $\mathbf{y}^*$  is an optimal solution of the dual problem  $D$ , then  $\mathbf{x}(\mathbf{y}^*)$  is the unique global optimal solution of  $P^{(k)}$ .*

A more circumstantial description of the Method of Moving Asymptotes can be found in e.g. [9]

### 3.3 Modifications of MMA

After having implemented The Method of Moving Asymptotes to the FFA-dynamic stall model the conclusion that the MMA did not converge for optimization problems without constraints could be drawn. Coming to this conclusion, the problem was solved by the following modifications made to MMA:

It can be shown that the problem

$$\min \sum_{i=1}^k \left( f_{i,\text{sim}}(\mathbf{x}) - f_{i,\text{exp}} \right)^2 \quad \text{when} \quad x_j^{\min} \leq x \leq x_j^{\max} \quad j = 1 \dots n$$

where  $k$  is the number of data points and  $n$  is the number of design variables, can equivalently, since it is a minimization problem, be written as

$$\min \sum_{i=1}^k \left( y_i^2 + z_i^2 \right)$$

provided that the following constraints are fulfilled:

$$f_{i,sim}(\mathbf{x}) - f_{i,exp} \leq y_i \quad i = 1 \dots k$$

$$y_i \geq 0 \quad i = 1 \dots k$$

$$-(f_{i,sim}(\mathbf{x}) - f_{i,exp}) \leq z_i \quad i = 1 \dots k$$

$$z_i \geq 0 \quad i = 1 \dots k$$

Exampel:

Assume  $(f_{i,sim}(\mathbf{x}) - f_{i,exp}) = 3$

Then from the four constraints above

$$y_i \geq 3, y_i \geq 0, \quad z_i \geq -3, \text{ and } z_i \geq 0$$

$$\Rightarrow y_i \geq 3 \text{ and } z_i \geq 0$$

This implies  $\min \sum_{i=1}^k (y_i^2 + z_i^2) = \{\min z_i \geq 0 \Rightarrow z_i = 0\} =$

$$= \min \sum_{i=1}^k (y_i^2 + 0) = \min \sum_{i=1}^k (f_{i,sim}(\mathbf{x}) - f_{i,exp})^2$$

This gives a problem with constraints and the modified MMA can now be implemented to the specific optimization problem with good convergence as a result.

### 3.4 Structure of the optimization program

In this chapter a brief description of the construction of the optimization program is presented.

The program is written in Visual Fortran 5.0 and a basic overview of the program structure and the subroutines included in the program can be seen below.

The optimization program:

**PROGRAM** FFA\_Dynopt

**Subroutine** Readin (Reads the input values)

**Subroutine** Objektfunc (Calculates the differentials)

**Subroutine** Dyncl (Calculates simulated  $C_l$ ,  $C_d$ , and  $C_m$ )

**Subroutine** Optimize (Calculates an optimal solution to the subproblem)

**Subroutine** Writeresult (Writes the result into files)

Central differences are used when the differentials, needed by the optimization routine, are calculated.

A flowchart for the optimization program can be seen in Appendix 2.

### 3.5 How to use the optimization program

A list of the input files is written in a file called Dynstallinput. All the input values needed by the optimization program are written in the input file named after the contents of the input file. The input values to the optimization program are among others convergence criteria, min-and max values of the design variables, names of the wind tunnel experiment data files, input values needed by the FFA dynamic stall model, static airfoil data etc.

In the input file the user can choose to run the optimization program in interactive mode, with the possibility to interrupt the optimization whenever satisfied, or batch mode and use the convergence criteria to interrupt the execution when the optimization is completed.





## 4 Optimization

In this chapter some optimization examples are presented and the results are analyzed.

Optimization has been made using wind tunnel experiments from three sources:

1. Ohio State University (OSU) [6].
2. Glasgow University (GU) [7].
3. Risoe [8].

and also results from Navier-Stokes calculation carried out at Risoe.

### 4.1 Cases of optimization and type of objective function

There are several ways of defining a relevant objective function.

A good agreement between experiments and simulations could be good agreement in maximum lift.

Since the average lift curve slope is very important for aerodynamic damping an objective function that considers the agreement in “ mean lift curve slope “ would also be possible.

In the current study objective function 2, equation (3.2), which is based on minimizing the deviation between experiments and simulations, was chosen.

$$f_2 = \sum_{i=1}^k \eta [(C_{n,sim}(t_i) - C_{n,exp}(t_i))^2] + \sum_{i=1}^k (1 - \eta) [(C_{t,sim}(t_i) - C_{t,exp}(t_i))^2]$$

By using different values of  $\eta$ , different weighting of normal and tangential force can be obtained.

In table 4.1 data for some cases used in the optimization is seen, for all cases see Appendix 3.

Table 1. Data for some cases for optimization.

Airfoil	Alfa mean	Alfa amplitude	Reduced frequency	Abbreviation
<b>Ohio State University. Wind tunnel pitching motion. Ref [ 6 ]</b>				
NACA 4415	14.2	10.8	0.046	n_m
LS(1) 0421 MOD	13.2	10.5	0.045	l_m
SERI 809	12.9	10.6	0.041	s_m
<b>Glasgow University. Wind tunnel pitching motion. Ref [ 7 ]</b>				
NACA 0015	11	7.6	0.102	N15_11_102
NACA 0021	11	7.8	0.097	N21_11_097
<b>Risoe- airfoil. Wind tunnel pitching motion. Ref [ 8 ]</b>				
Risoe-1	11.8	1.6	0.11	dclm02dcdm007
<b>Risoe- airfoil. CFD calculations.</b>				
Plunging	11.8	1.6	0.11	CFD Plunging
Pitching	11.8	1.6	0.11	CFD Pitching

## 4.2 Effect of small errors in wind tunnel measurements

When the optimization program is run for measurements from Risoe with mean angle of attack of  $11.8^\circ$  the optimized semi-empirical parameters become  $T_v=6.2$  and  $T_f=0.8$ . Such a low value of  $T_f$  can not be seen in the optimization for other airfoils and considering the physical interpretation of the delay in the separation point, this  $T_f$  value is too low.

A second optimization was therefore made with the dynamic wind tunnel data shifted in the  $C_l$  direction, this case is abbreviated dclm02dcdm007. A shift of  $\Delta C_l = -0.02$ , which seemed quite reasonable, was applied to the dynamic wind tunnel data before the optimization program was run. The result was quite different from the foregoing with the following optimized values:  $T_v=1.2$  and  $T_f=4.2$ .

This shows that possible errors in the experiments have a large impact on the optimized values of the semi-empirical parameters  $T_f$  and  $T_v$ .

In Fig. 4.2,  $Cl(\alpha)$  and  $Cd(\alpha)$  are plotted for original wind tunnel data as well as for the case with a shift in the  $C_l$  direction. In the figure one can see that the model is quite good at predicting the measured force coefficients for the shifted case as well as for the non-shifted case, even though the optimization result in different parameter values.

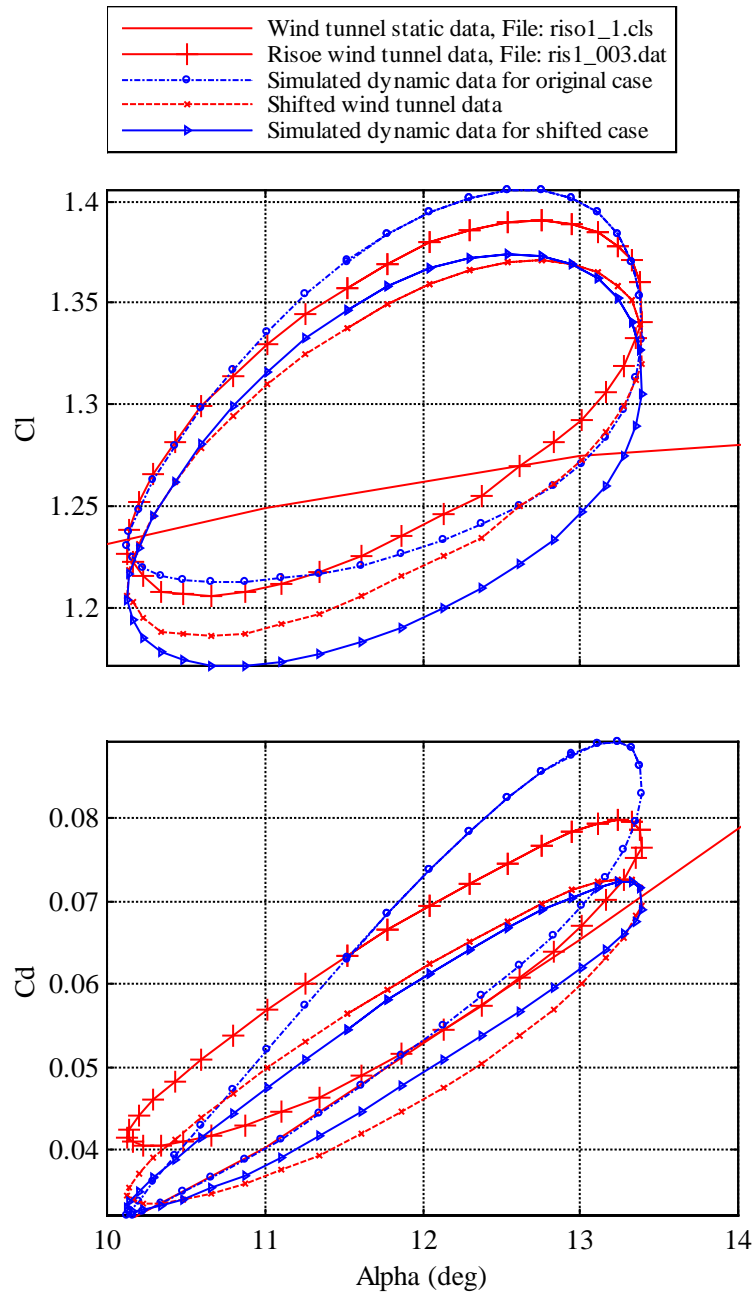


Figure 4.1 Results from calculations on data from Risoe, Risoe-1.  $\alpha$  - mean= $11.8^\circ$ ,  $\alpha$  - amplitude= $1.6^\circ$  and  $k=0.11$ . Optimized semi-empirical parameters with  $\eta=0.1$  for original case:  $T_v=6.2$ ,  $T_f=0.84$  and  $acd=0.023$ . Optimized semi-empirical parameters with  $\eta=0.1$  for shifted case:  $T_v=1.2$ ,  $T_f=4.18$  and  $acd=0.001$ .

### 4.3 Optimization Results

Some of the different cases and the corresponding values for optimized parameters are shown in the tables below. The results for all the cases can be seen in Appendix 4.

Table 4.2. Optimized result for three design variables and  $\eta=0.1$ .

Case	Optimized		
	Tv	Tf	acd
n_m	2.71	3.9	0.0094
l_m	0.89	6.95	0.0001
s_m	1.6	5.34	0.11
N15_11_102	6.26	7.39	0.165
N21_11_097	3.65	8.66	0.14
dclm02dcdm007	1.21	4.18	0.0001
CFD Plunging	0.0001	8.66	0.0001
CFD Pitching	1.37	1.44	0.1

Table 4.3. Optimized result for three design variables and  $\eta=0.5$ .

Case	Optimized		
	Tv	Tf	acd
n_m	2.7	3.93	0.019
l_m	3.91	3.46	0.15
s_m	0.0001	7.03	0.011
N15_11_102	3.13	10.43	0.11
N21_11_097	2.6	10	0.11
dclm02dcdm007	1.74	3.47	0.0001
CFD Plunging	0.0001	8.23	0.013
CFD Pitching	1.28	1.55	0.12

From tables 4.2 and 4.3 above, optimization with three design variables, tables 4.4 and 4.5 next page, optimization with four design variables, one can see that the semi-empirical parameters varies quite much for the different cases. This holds both for optimization with  $\eta=0.1$  and optimization with  $\eta=0.5$  in the objective function (eq. 3.2). It is difficult to see any pattern between optimized semi-empirical parameters for optimization with  $\eta=0.1$  as well as for  $\eta=0.5$ .

Table 4.4 Optimized result for four design variables and  $\eta=0.1$ 

Case	Optimized			
	Tv	Tf	acd	Tp
n_m	2.9	4.35	0.032	0.0001
l_m	1.04	7.51	0.01	0.0001
s_m	2.2	5.46	0.15	0.0048
N15_11_102	7.55	5.27	0.1	3.44
N21_11_097	0.0001	6.35	0.079	3.48
dclm02dcdm007	1.38	4.94	0.0001	0.0001
CFD Plunging	0.0001	9.53	0.001	0.0001
CFD Pitching	1.38	2.24	0.11	0.0001

Table 4.5 Optimized result for four design variables and  $\eta=0.5$ 

Case	Optimized			
	Tv	Tf	acd	Tp
n_m	2.69	4.03	0.018	0.68
l_m	3.74	4.34	0.15	0.0001
s_m	0.0001	7.58	0.005	0.0001
N15_11_102	0.0001	7.91	0.06	3.63
N21_11_097	0.0001	6.6	0.063	4
dclm02dcdm007	1.82	4.31	0.0001	0.0001
CFD Plunging	0.0001	9.04	0.016	0.0001
CFD Pitching	1.11	2.56	0.09	0.0001

In the following figures the results from the calculations are plotted. In each figure the load coefficients  $C$ ,  $C_n$ ,  $C$  and  $C_x$  vs. angle of attack  $\alpha$  are plotted. In figures 4.3-4.8 one can see comparisons between simulations with a set of reference parameter values and simulations with optimized parameter values for some cases. Using the reference parameters  $Tv=2$ ,  $Tf=5$  and  $acd=0.08$  in the model one can get a reasonably good agreement, between measured and simulated data, for a large number of cases, particularly OSU cases. In fig. 4.9-4.14 comparison between simulations with optimized parameter values achieved using  $\eta=0.1$  and  $\eta=0.5$ , in the objective function, are seen.

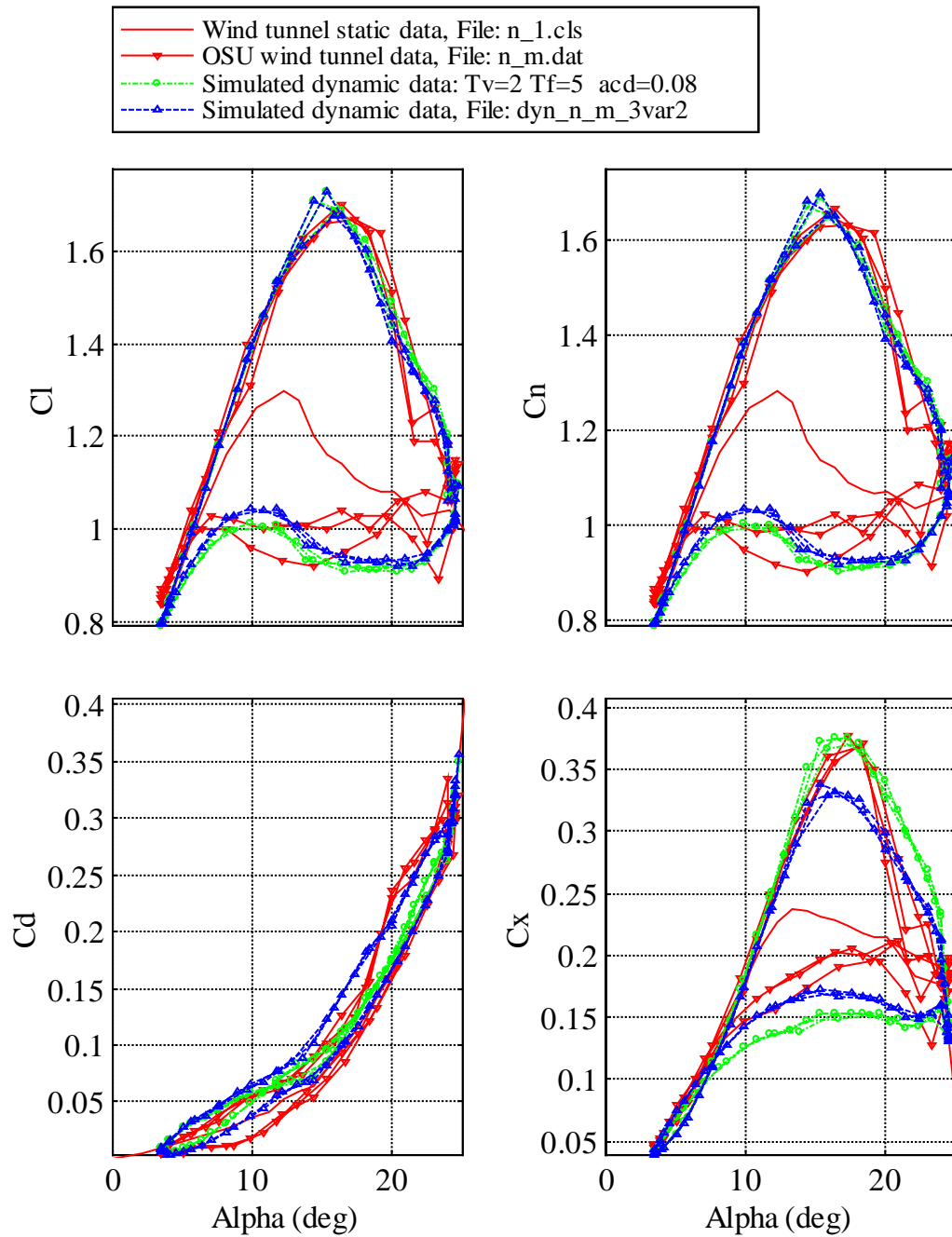


Fig. 4.3 Results from calculations on data from OSU, NACA 4415, medium frequency.  $\eta=0.1$ . Optimized semi-empirical parameters:  $T_v=2.71$ ,  $T_f=3.9$  and  $acd=0.0094$ .

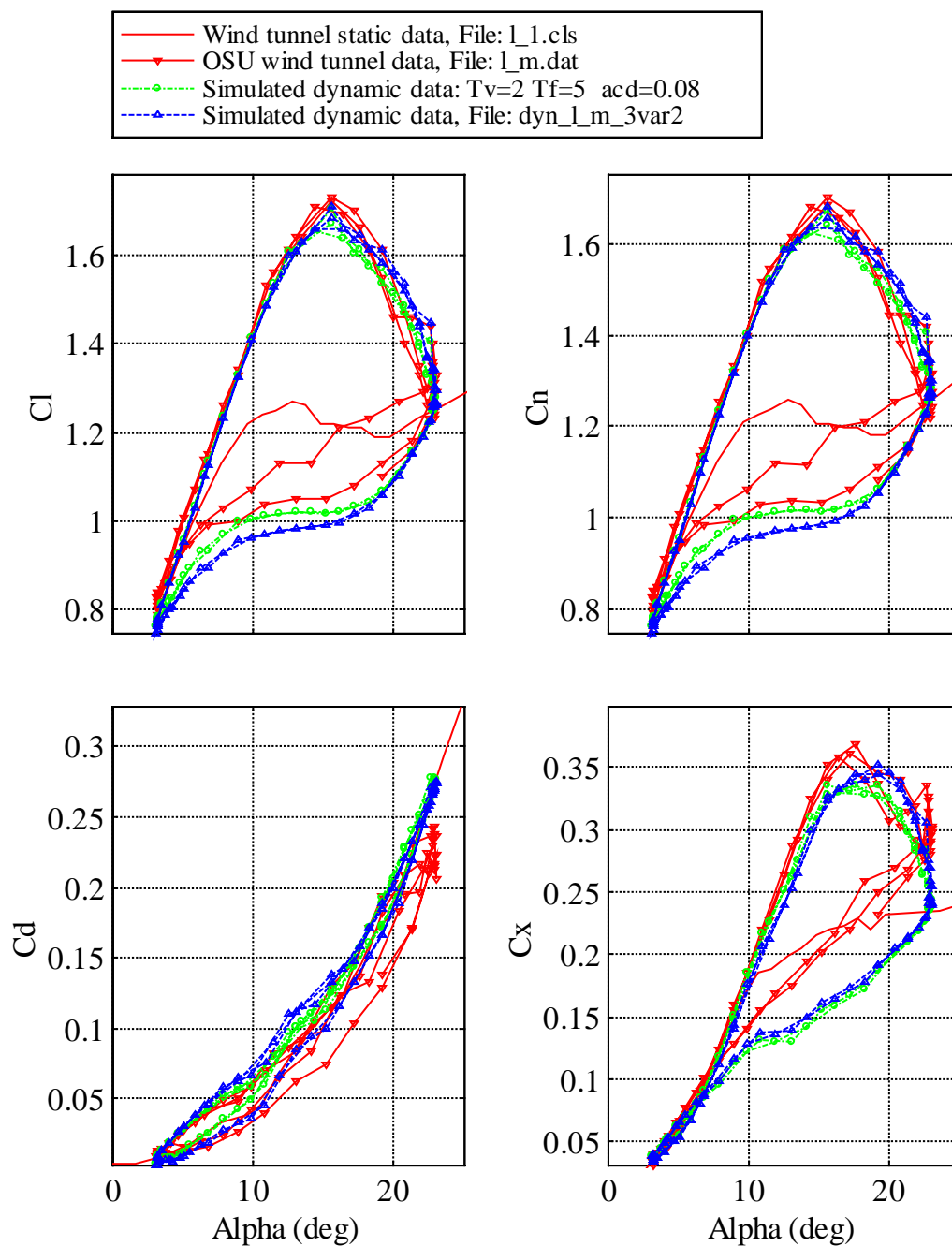


Fig. 4.4 Results from calculations on data from OSU, LS (1) 0421 MOD, medium frequency.  $\eta=0.1$  Optimized semi-empirical parameters:  $T_v=0.89$ ,  $T_f=6.95$  and  $acd=0.001$ .

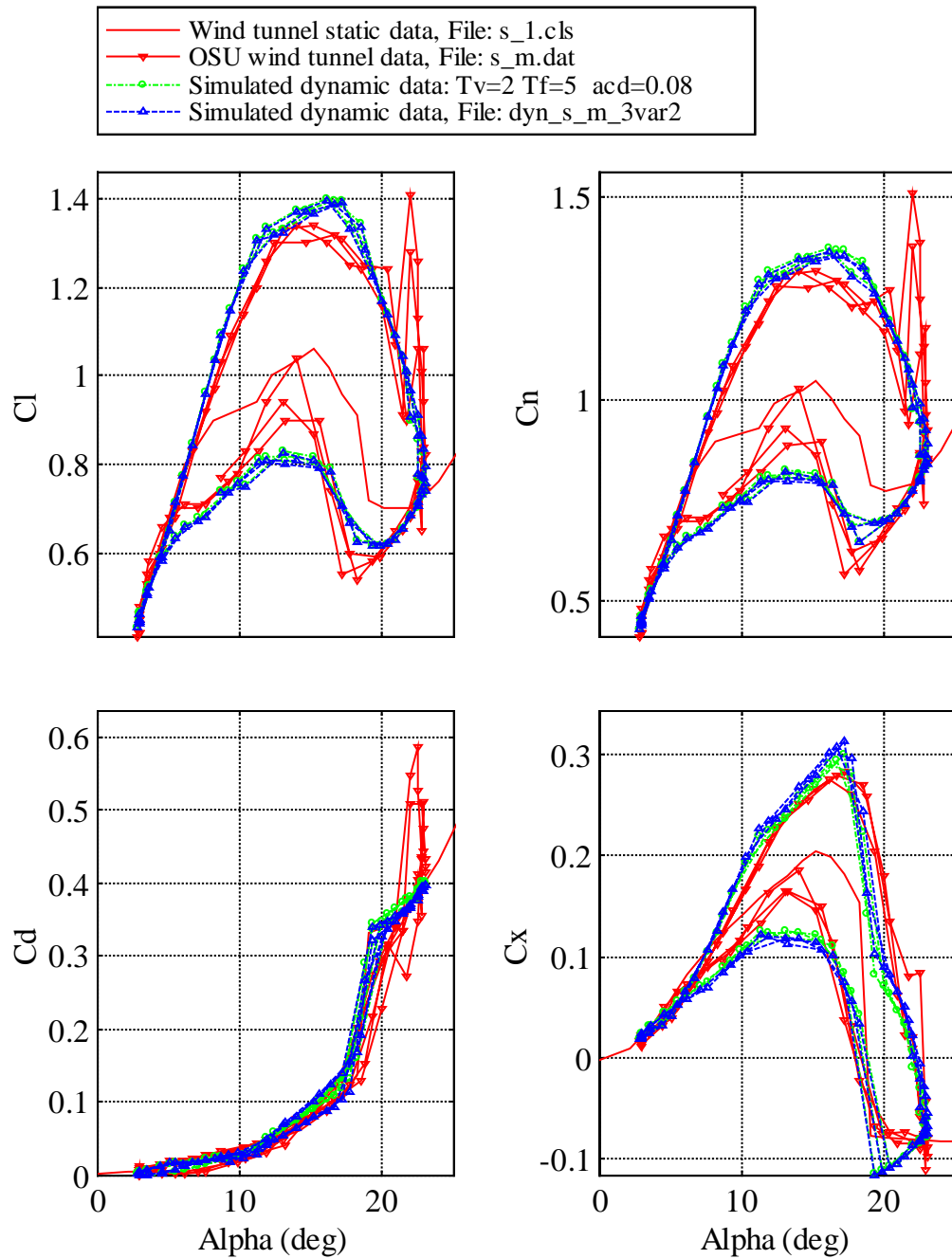


Fig.4.5 Results from calculations on data from OSU, SERI 809, medium frequency.  $\eta=0.1$  Optimized semi-empirical parameters:  $T_v=1.6$ ,  $T_f=5.34$  and  $acd=0.11$ .



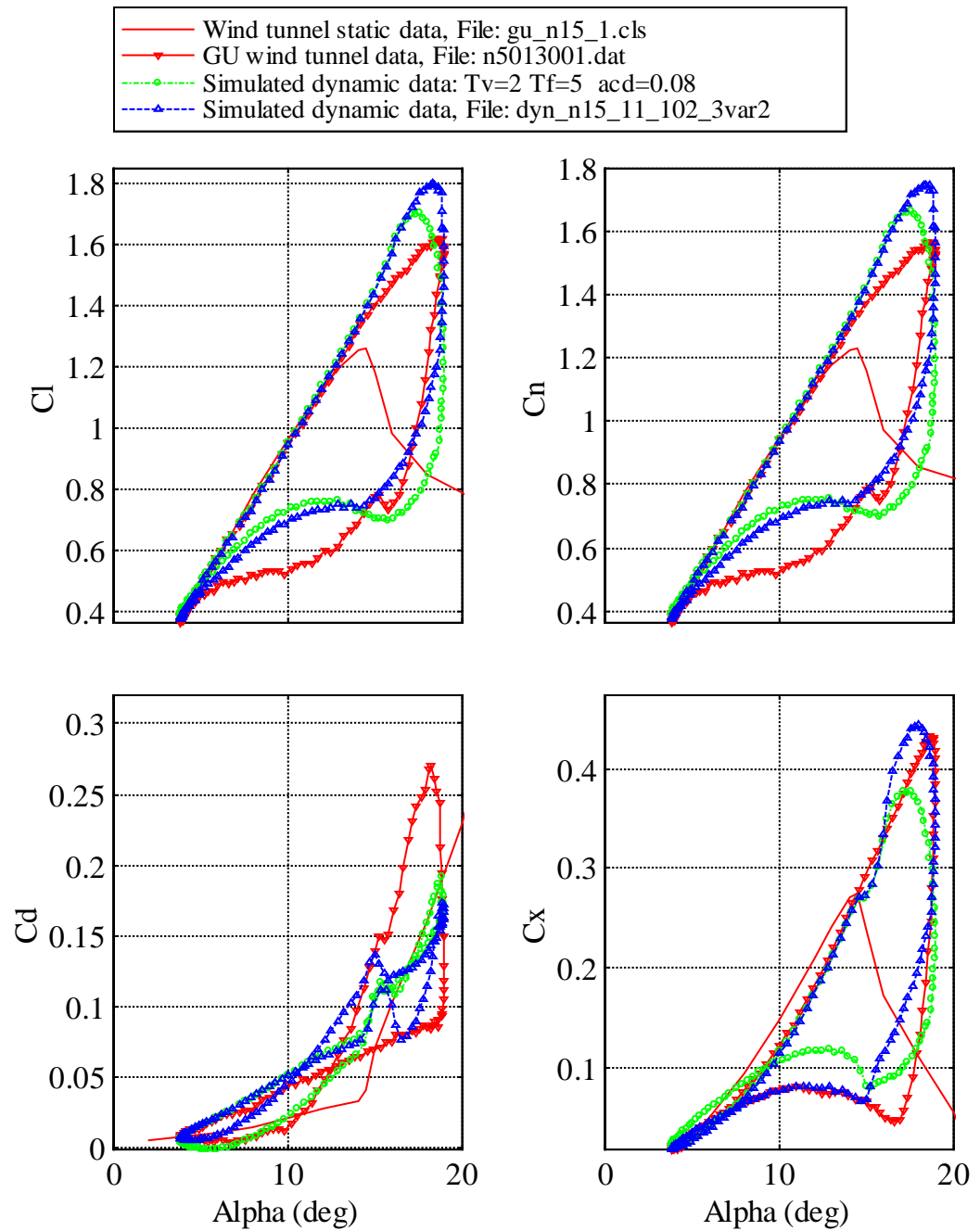


Fig.4.6 Results from calculations on data from GU, NACA 0015, reduced frequency=0.102.  $\eta = 0.1$  Optimized semi-empirical parameters:  $T_v=6.26$ ,  $T_f=7.39$  and  $acd=0.165$ .

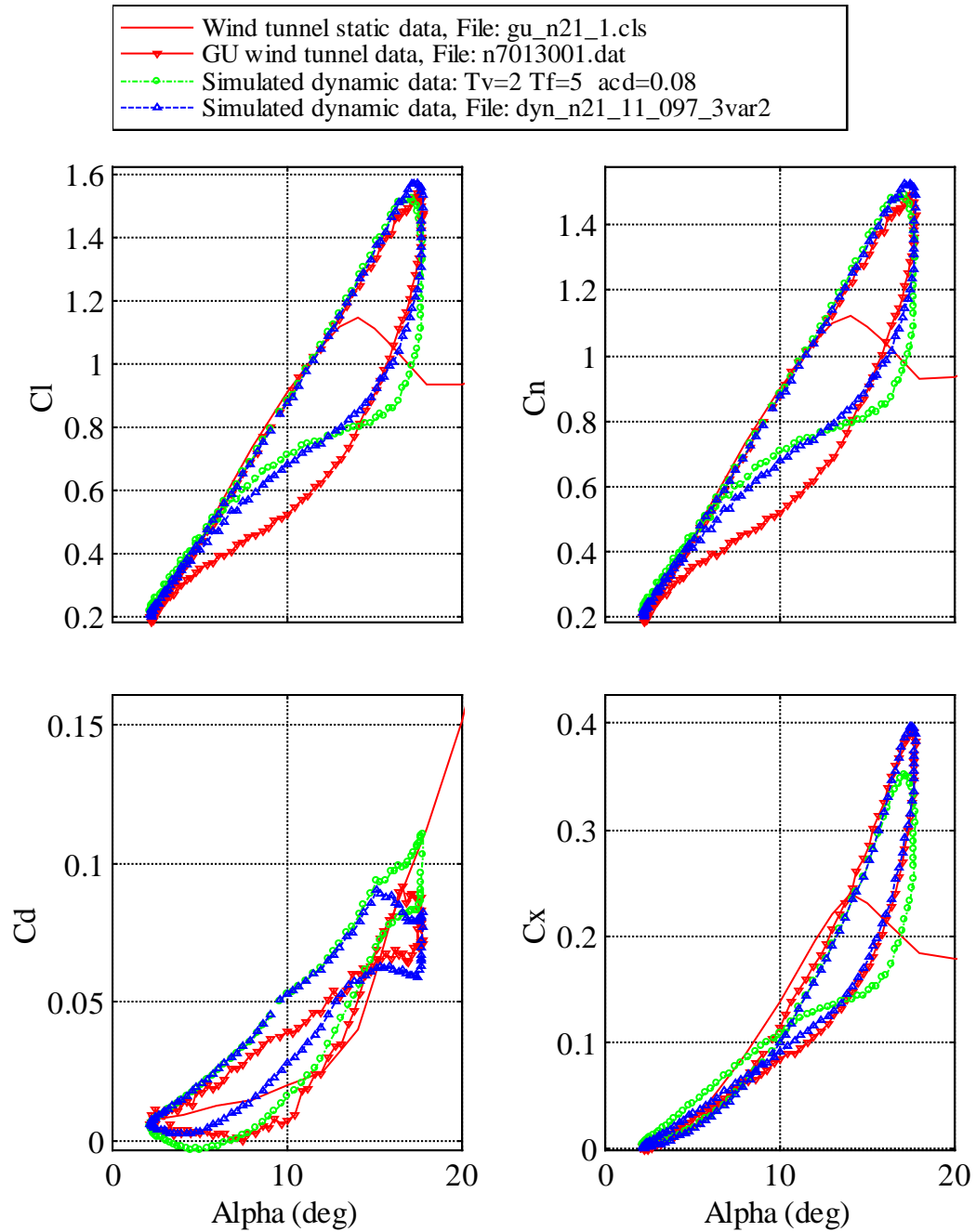


Fig. 4.7 Results from calculations on data from GU, NACA 0021, reduced frequency=0.097.  $\eta=0.1$ . Optimized semi-empirical parameters:  $T_v=3.65$ ,  $T_f=8.66$  and  $acd=0.14$ .

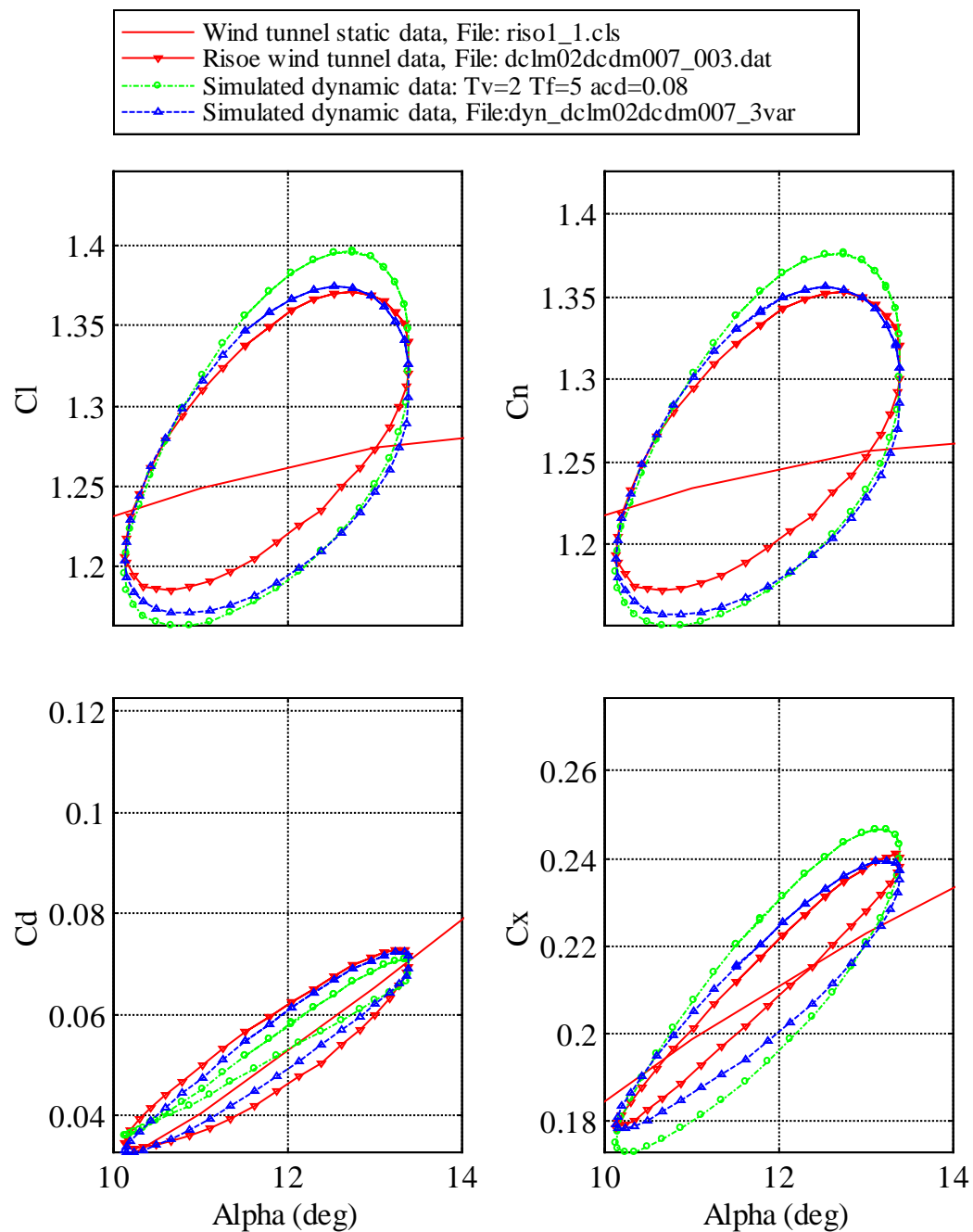


Fig.4.8 Results from calculations on data from Risoe, Risoe-1.  $\eta=0.1$  Optimized semi-empirical parameters:  $T_v=1.21$ ,  $T_f=4.18$  and  $acd=0.0001$ .

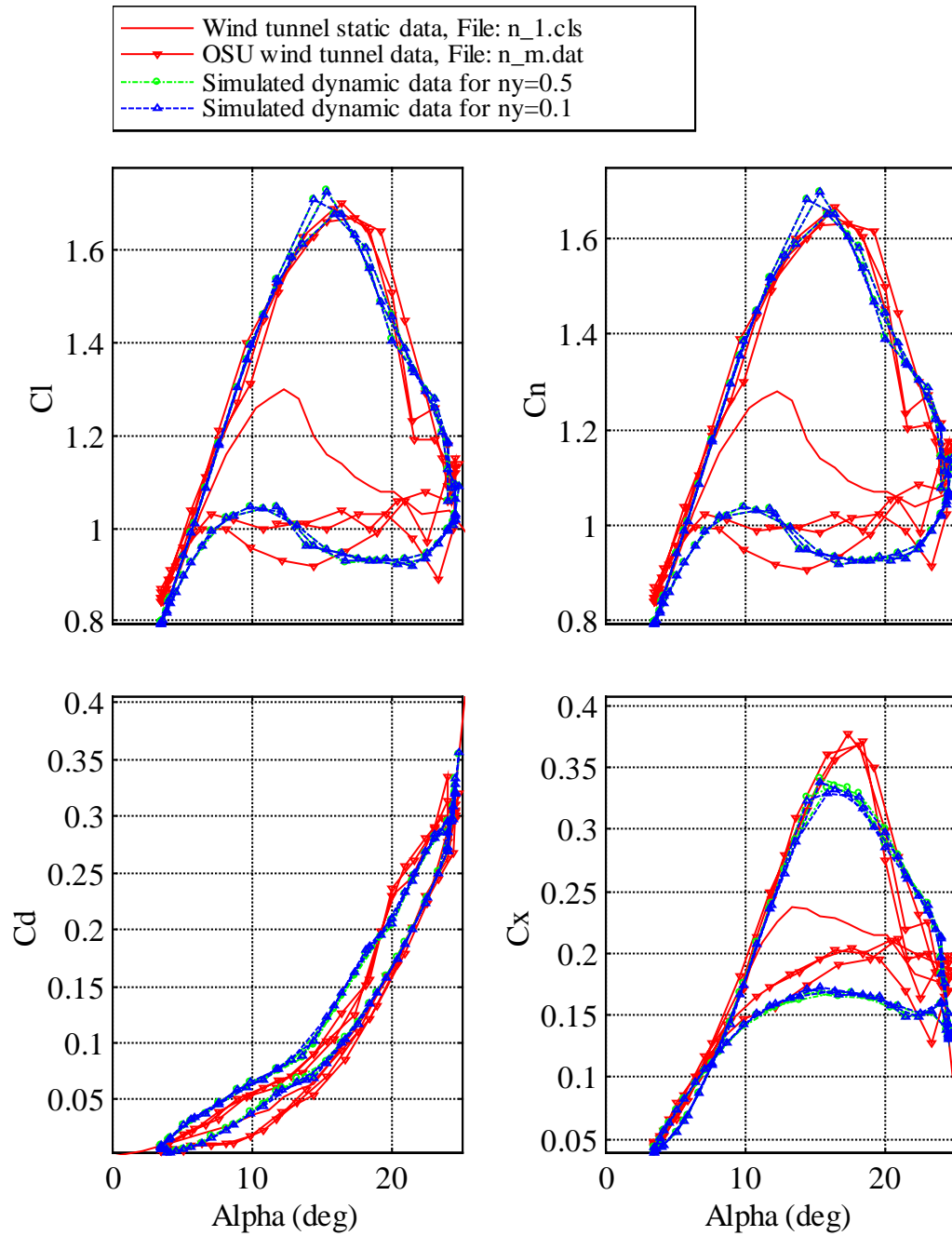


Fig. 4.9 Results from calculations on data from OSU, NACA 4415, medium frequency. Comparison of optimization with  $\eta=0.5$  and  $\eta=0.1$ .

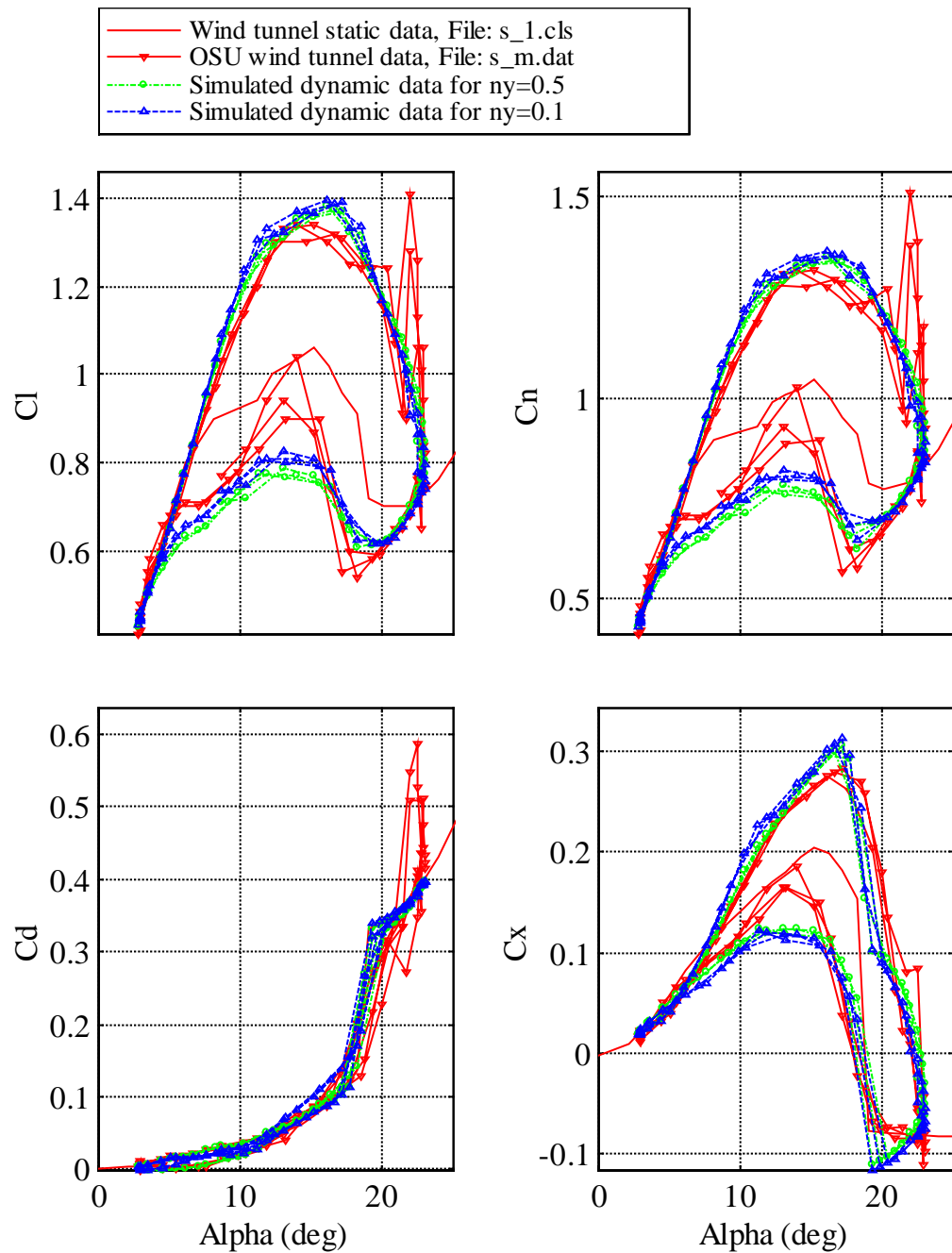


Fig. 4.10 Results from calculations on data from OSU, LS (1) 0421 MOD, medium frequency. Comparison of optimization with  $\eta=0.5$  and  $\eta=0.1$ .

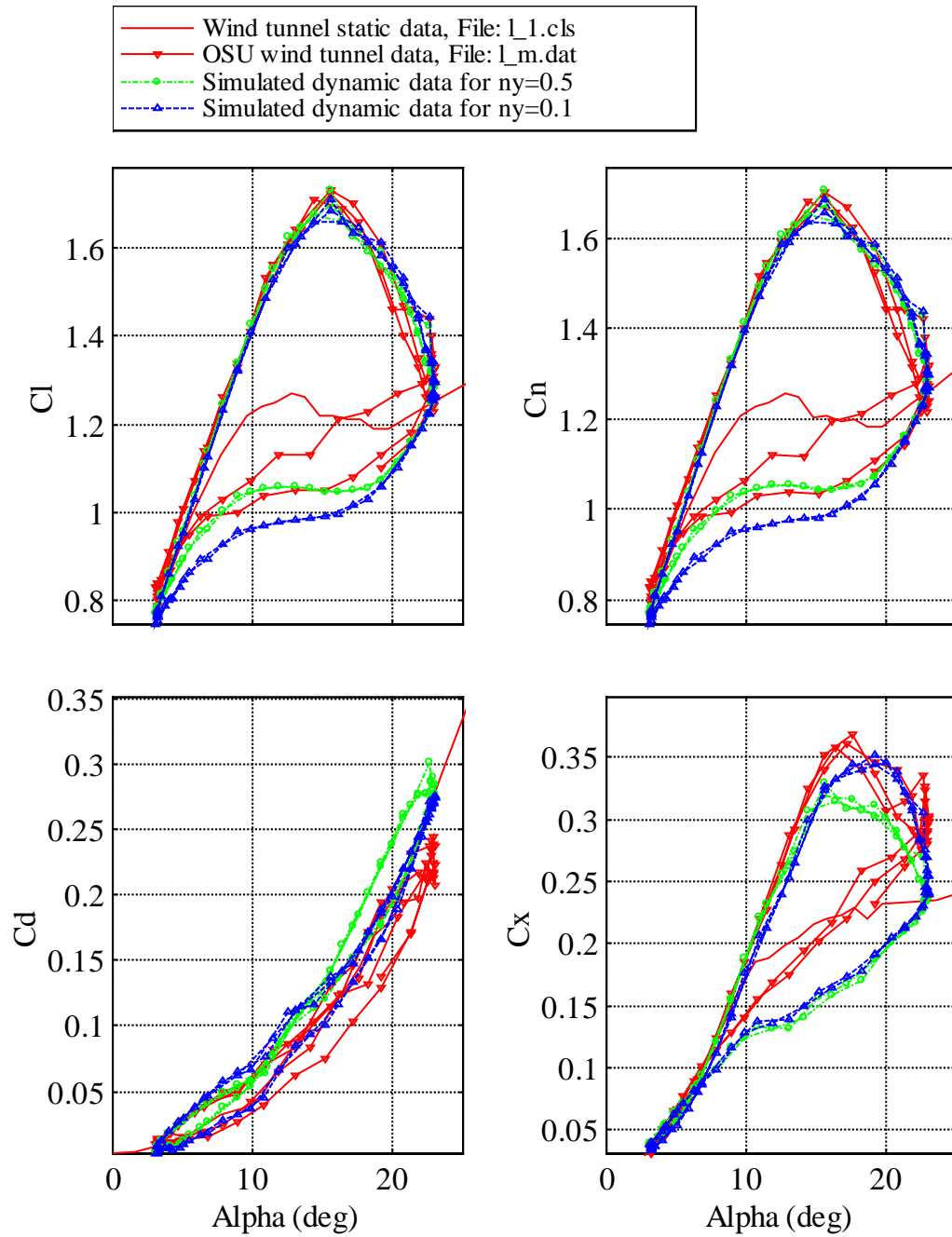


Fig.4.11 Results from calculations on data from OSU, SERI 809, medium frequency. Comparison of optimization with  $\eta=0.5$  and  $\eta=0.1$ .

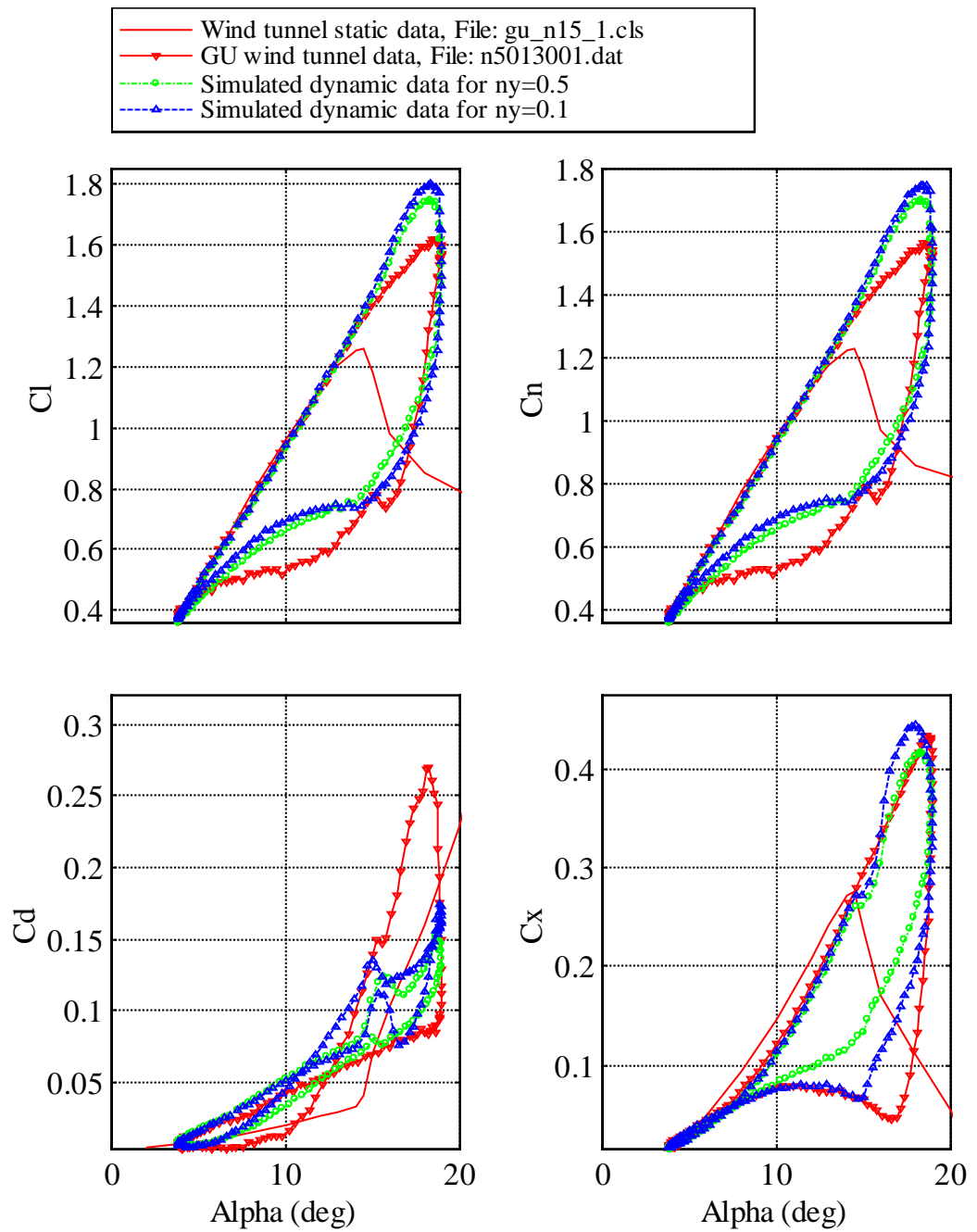


Fig.4.12 Results from calculations on data from GU, NACA 0015, reduced frequency=0.102. Comparison of optimization with  $\eta=0.5$  and  $\eta=0.1$ .

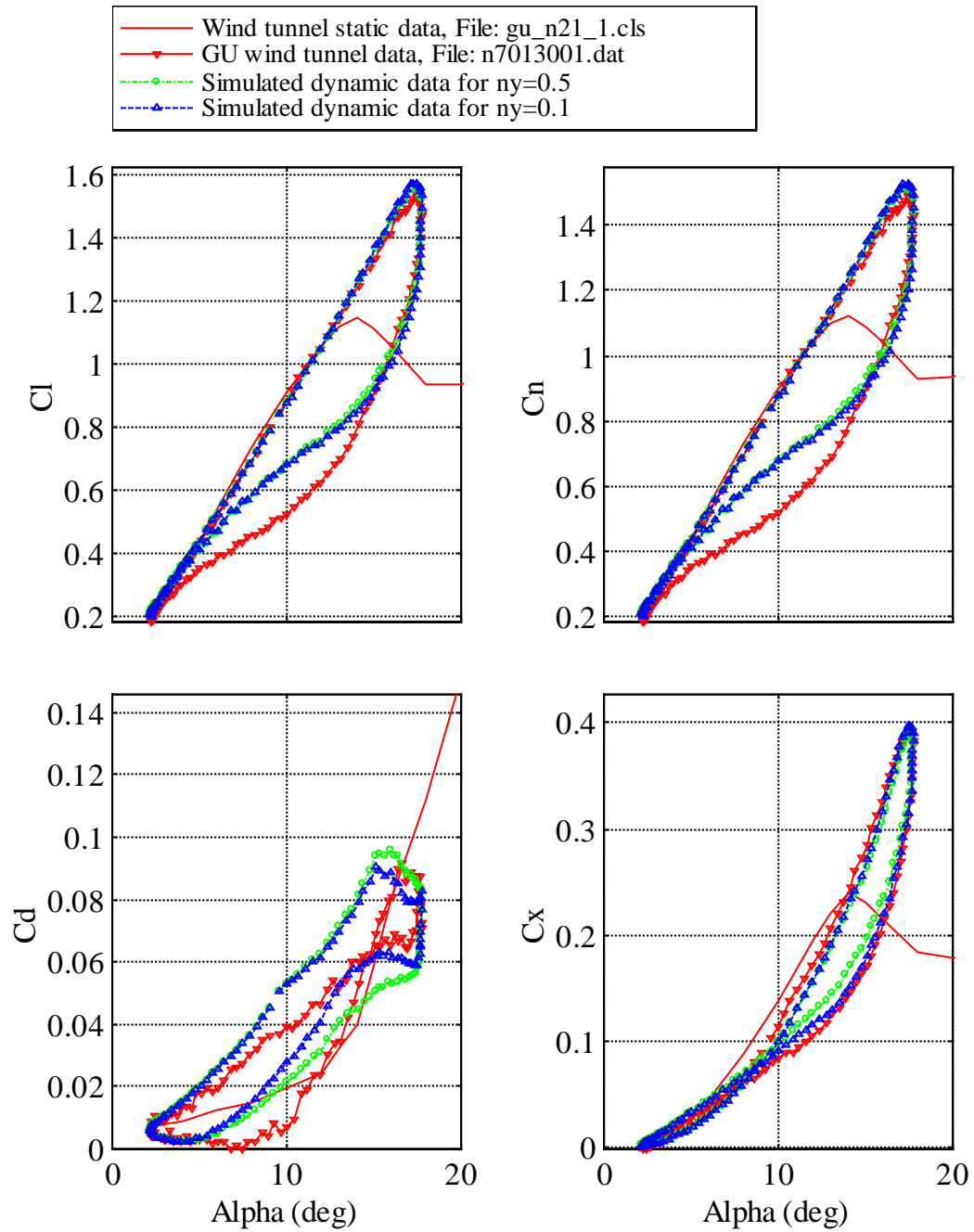


Fig. 4.13 Results from calculations on data from GU, NACA 0021, reduced frequency=0.097. Comparison of optimization with  $\eta=0.5$  and  $\eta=0.1$ .



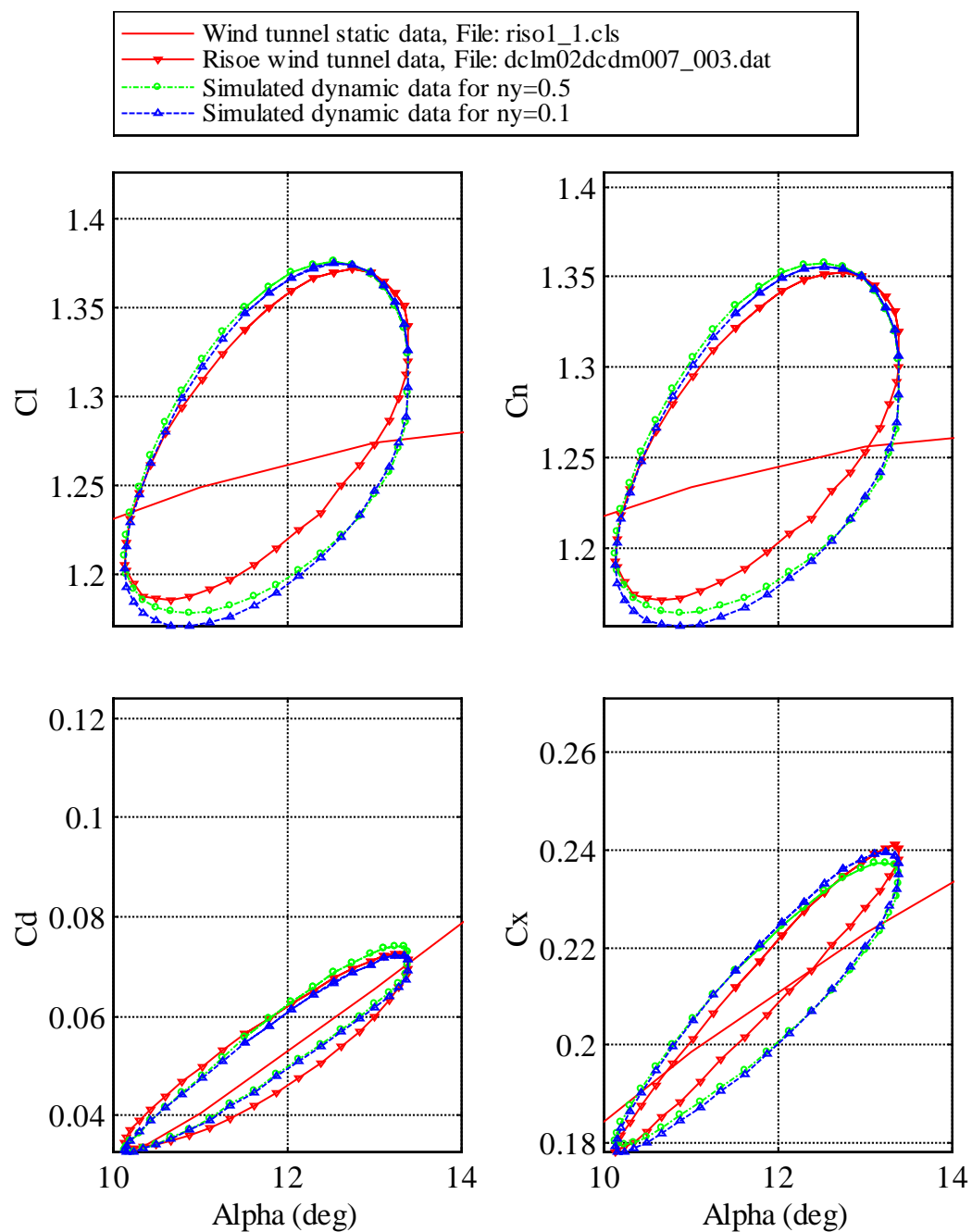


Fig.4.14 Results from calculations on data from Risoe, Risoe-1. Comparison of optimization with  $\eta=0.5$  and  $\eta=0.1$ .

### 4.3.1 Results from CFD

Navier-Stokes calculations with the Risoe Ellipsys code with a  $k-\omega$  SST turbulence model was done for the Risoe-1 airfoil. These calculations were made at the same reduced frequency and  $\alpha$ -amplitude as the wind tunnel test with mean- $\alpha$  of  $11^\circ$ . The calculations were done with the airfoil in pitching motion with amplitude of  $1.6^\circ$  and also with the airfoil in plunging motion. For plunging motion the plunging amplitude was set to  $h/c=0.127 \sin(\omega t)$  corresponding to the same  $\alpha$ -amplitude as for the pitching case.

Comparing the results for pitching and plunging motion it can be seen that the mean lift curve slope is larger for the plunging case, which is opposite to what is found from analysis of pitching and plunging motion of wind turbine blade in the wind tunnel test analyzed in [7]

Comparing the wind tunnel pitching motion results and CFD pitching calculations, it can be seen that the CFD results show a much smaller mean lift curve slope and that the width of the loop is smaller. This is also reflected in the resulting optimized value of  $Tf$ , which is smaller for the CFD case.

As can be seen in figures 4.15-4.18 the dynamic stall model can mimic the wind tunnel and CFD results quite well, as long as the used semi-empirical parameters are optimized for the specific case. The variation in optimized semi-empirical parameters, however, are different for the two cases and it is difficult to select one set of values that would be representative for the airfoil without having an idea of which case to trust the most.

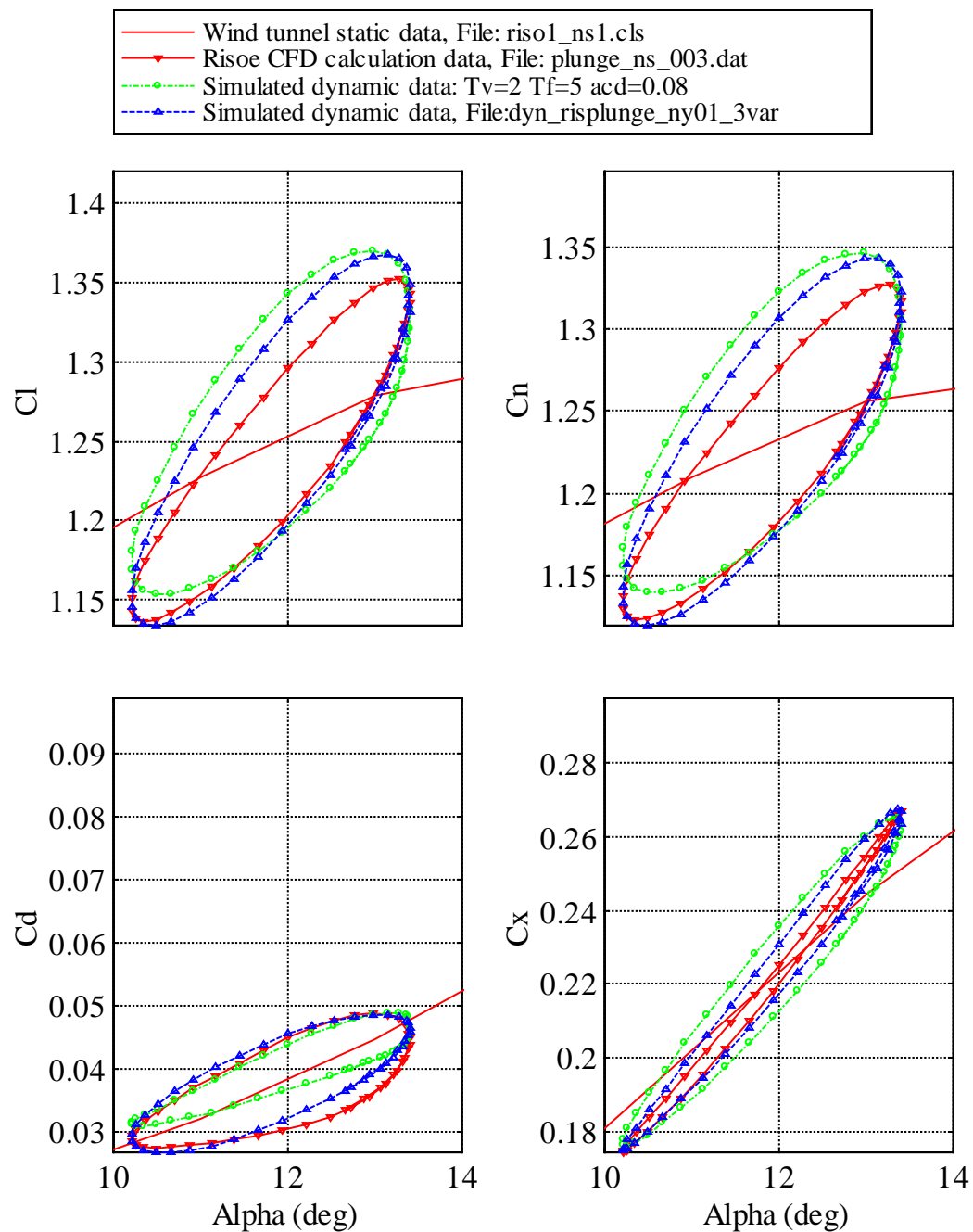


Fig.4.15 Results from calculations on CFD data from Risoe, plunging motion.  $\eta=0.1$   
Optimized semi-empirical parameters:  $T_v=0.0001$ ,  $T_f=8.66$  and  $acd=0.0001$ .

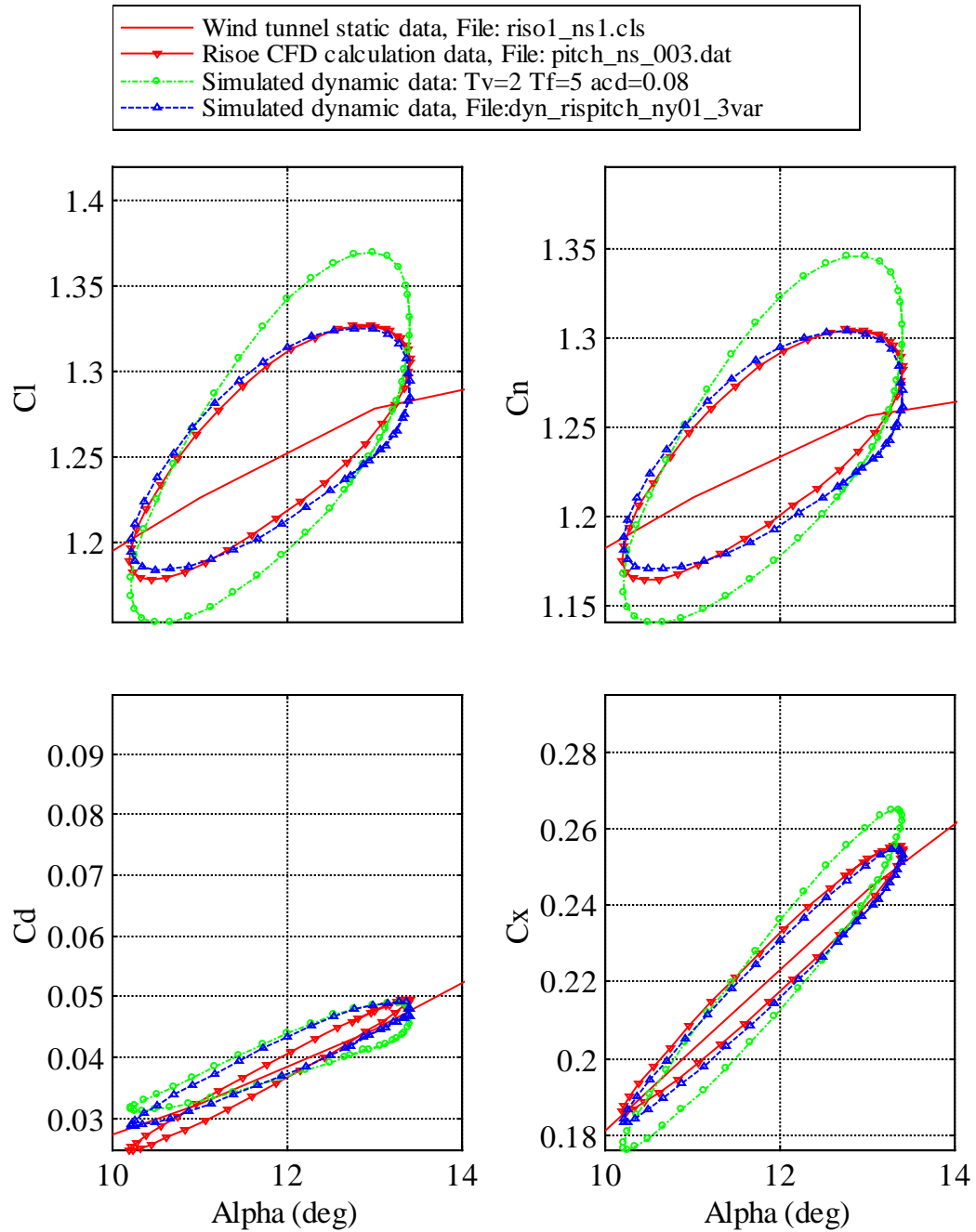


Fig.4.16 Results from calculations on CFD data from Risoe, pitching motion.  $\eta=0.1$ . Optimized semi-empirical parameters:  $T_v=1.37$ ,  $T_f=1.44$  and  $acd=0.1$ .

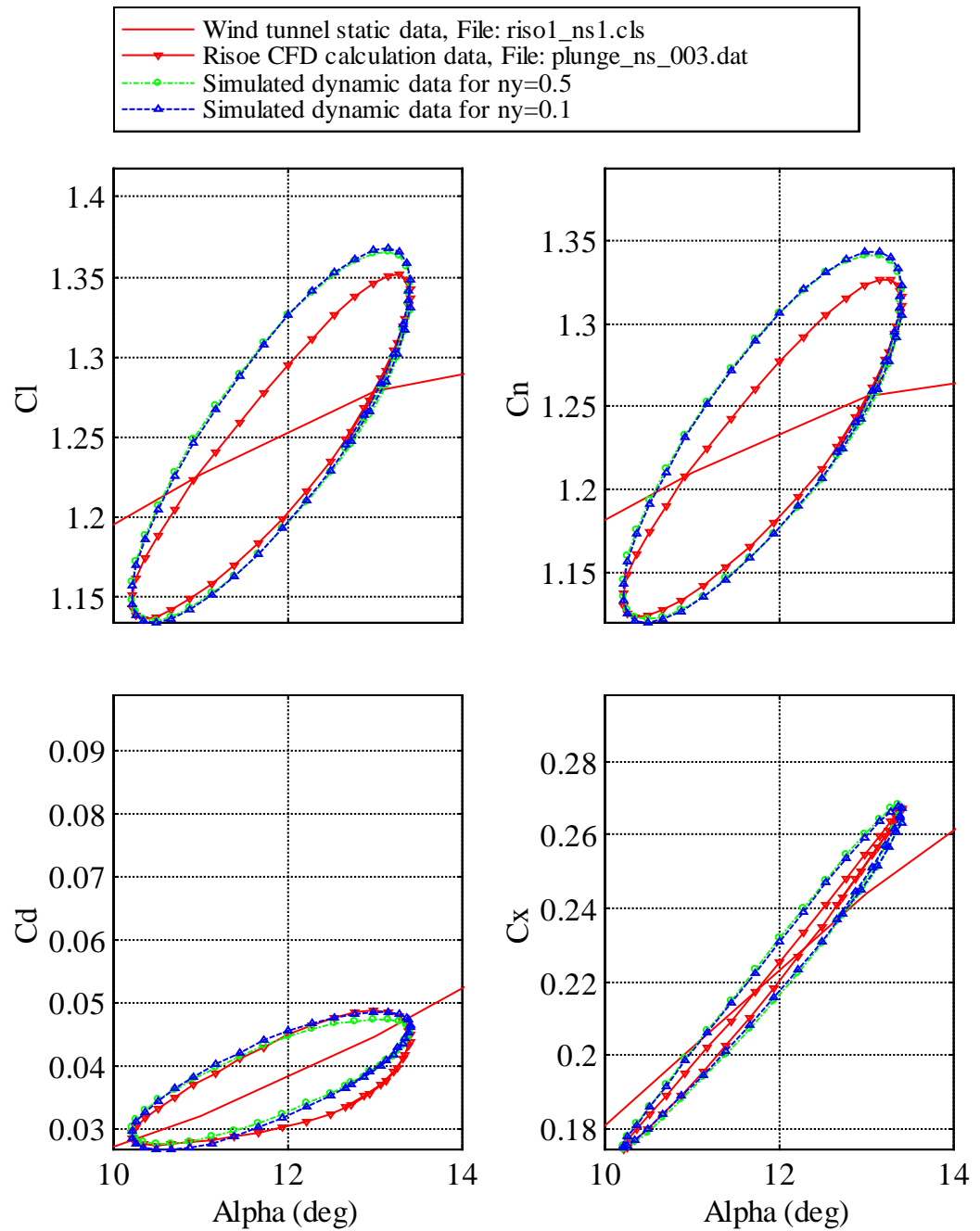


Fig.4.17 Results from calculations on CFD data from Risoe, plunging motion. Comparison of optimization with  $\eta=0.5$  and  $\eta=0.1$ .

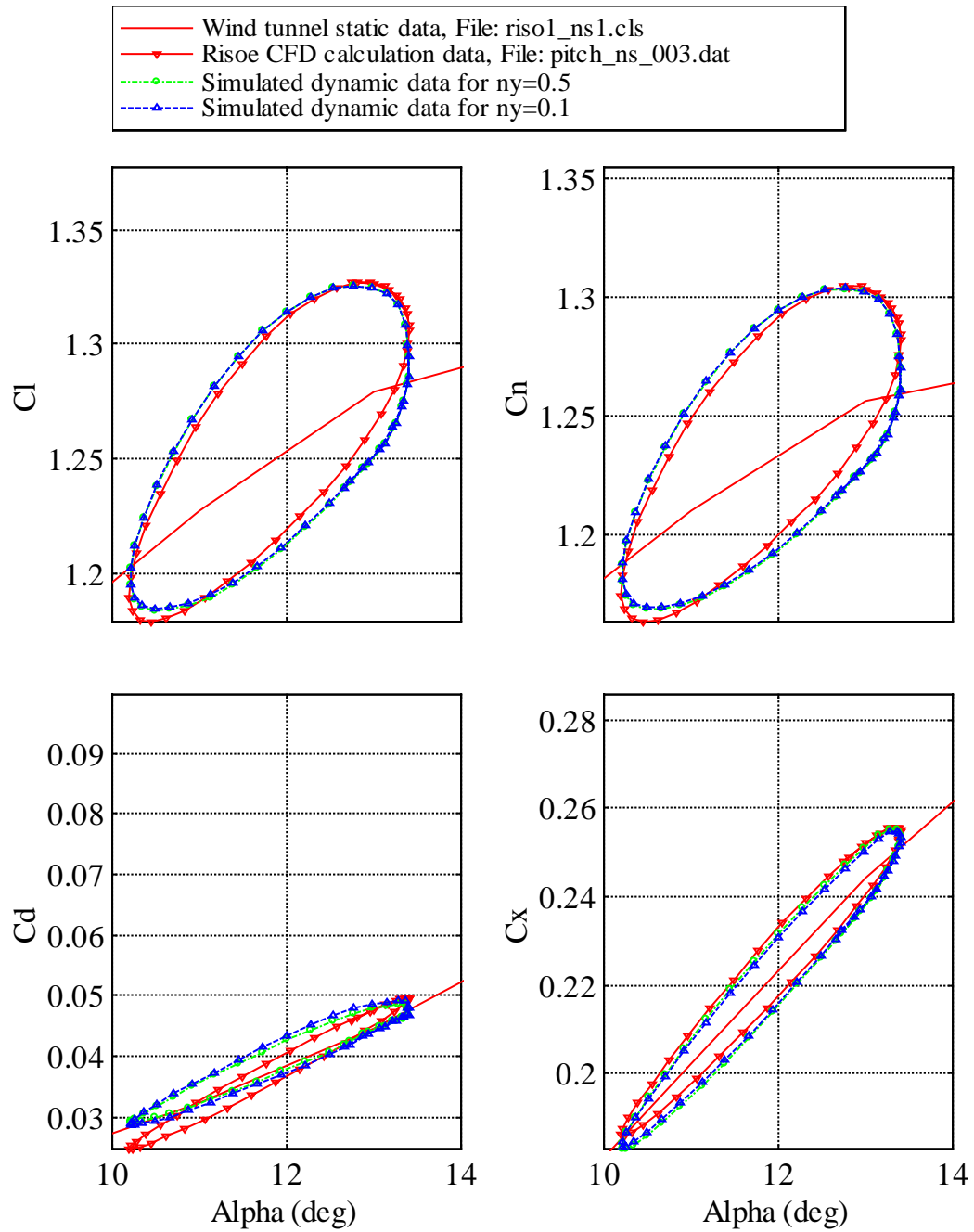


Fig.4.18 Results from calculations on CFD data from Risoe, pitching motion. Comparison of optimization with  $\eta=0.5$  and  $\eta=0.1$ .

## 4.4 Shortcoming of the dynamic stall model

The usefulness of the semi-empirical dynamic stall model is dependent on that physical mechanisms of dynamic stall are correctly enough described. For experiments with high mean- $\alpha$  and high amplitudes, especially cases from Glasgow University, one can in the measurements see a marked vortex shedding process with multiple vortices. This is not sufficiently modeled by the FFA-Beddoes dynamic stall model since the currently used model, has no criterion for the start of "vortex travelling", and vortex contribution is allowed as long as the angle of attack is increasing, see Fig. 4.19–4.20 below.

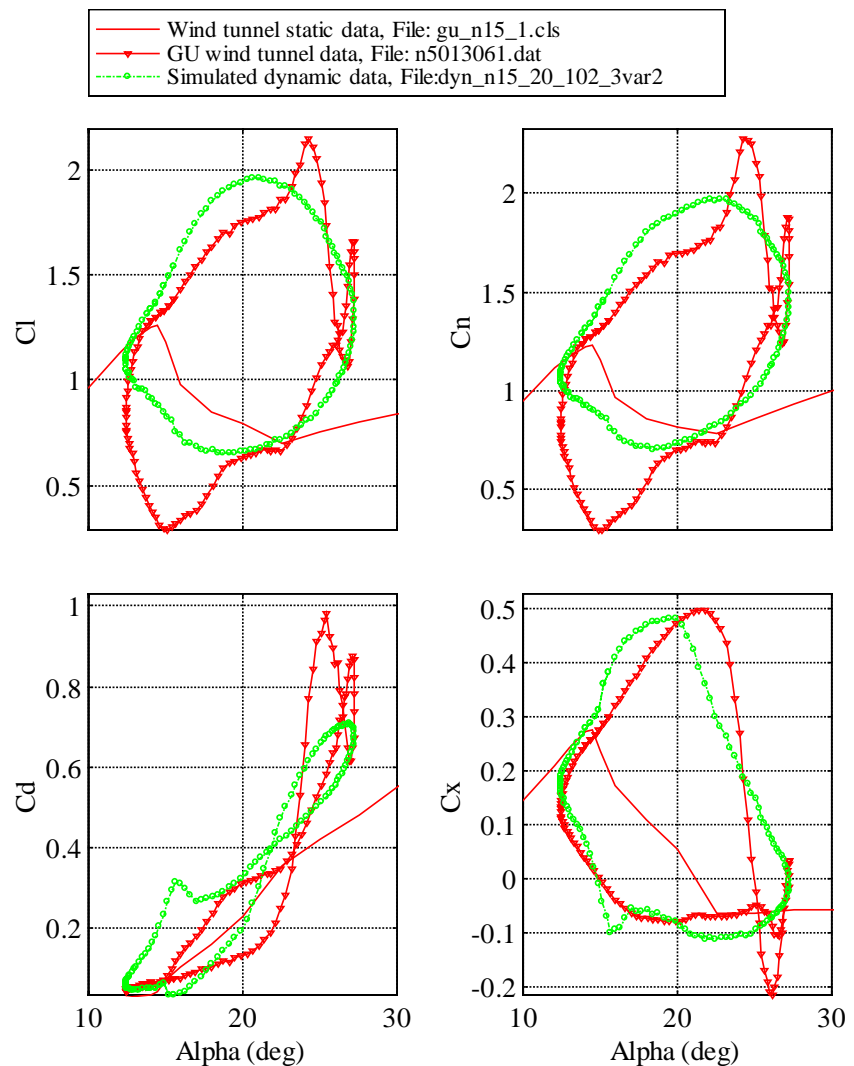


Fig.4.19. Results from calculations on data from GU, NACA 0015.  $\alpha$  - mean=19.8°,  $\alpha$  -amplitude=7.4° and reduced frequency =0.102.  $\eta$ =0.1.

Optimized semi-empirical parameters:  $T_v=4.91$ ,  $T_f=8.82$  and  $acd=0.0001$ .

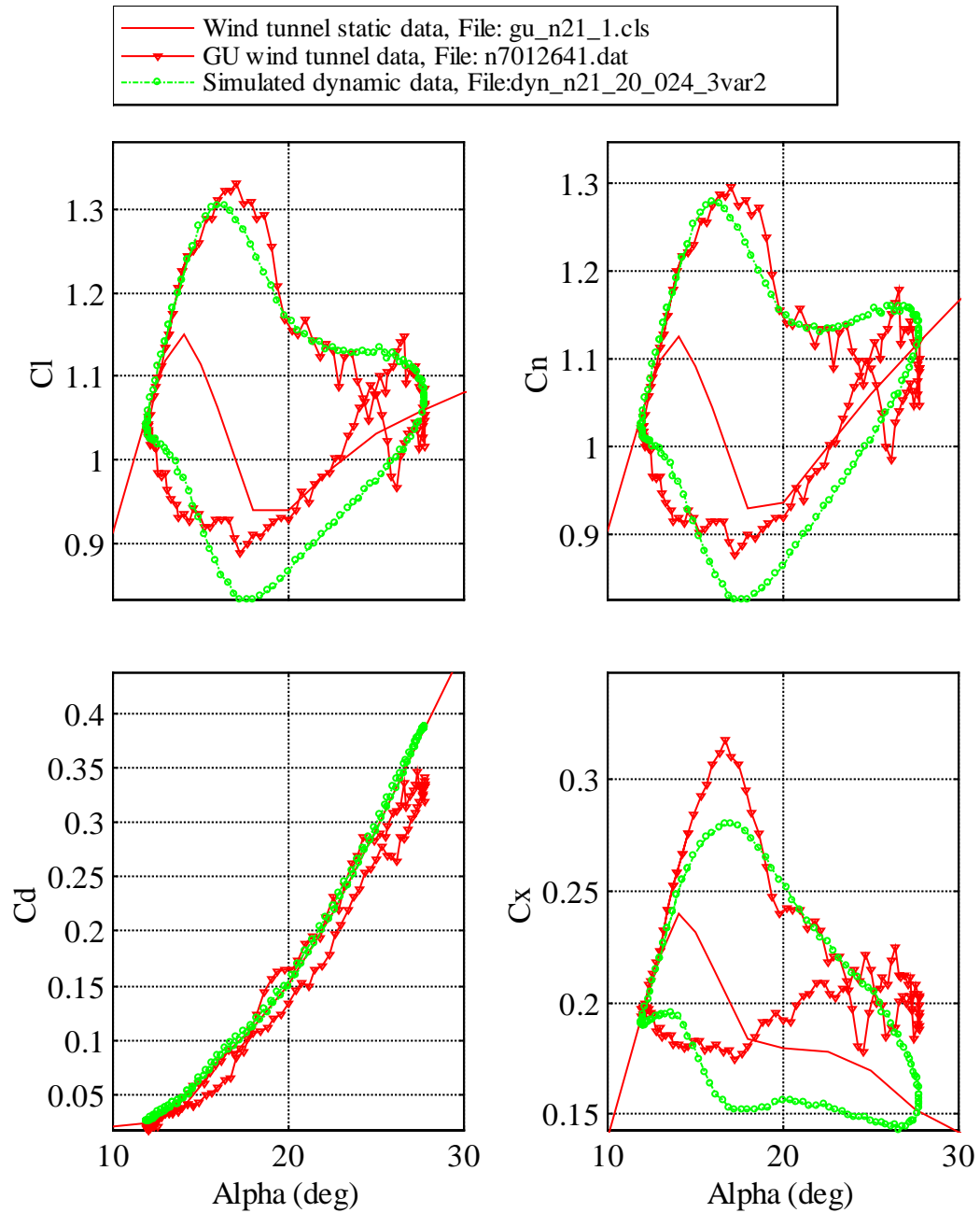


Fig.4.20. Results from calculations on data from GU, NACA 0021.  $\alpha$  - mean= $19.9^\circ$ ,  $\alpha$  -amplitude= $7.9^\circ$  and reduced frequency =0.24.  $\eta=0.1$ . Optimized semi-empirical parameters:  $T_v=1.36$ ,  $T_f=8.91$  and  $acd=0.027$ .



## 4.5 The Root Mean Square function and Comparison between different cases.

The optimization is made for different numbers of data points for different cases. It is quite difficult to compare the value of the objective function for different cases. In an attempt to simplify the problem and to be able to compare the value of the objective functions, the RMS function was introduced.

$$RMS = \sqrt{\frac{\eta \cdot \sum_{i=1}^k [(C_{n,sim}(t_i) - C_{n,exp}(t_i))^2]}{k}} + \sqrt{\frac{(1-\eta) \cdot \sum_{i=1}^k [(C_{t,sim}(t_i) - C_{t,exp}(t_i))^2]}{k}} \quad (4.2)$$

To get a survey of the objective functions the RMS function was plotted against Tf and Tv. As one can see in Fig 4.1 below the RMS function is very smooth and rather flat. At the minimum point about Tv=3.5 and Tf=3.8 the RMS value is quite insensitive to changes in Tf and Tv.

These conclusions give us a hint about the actual optimization problem.

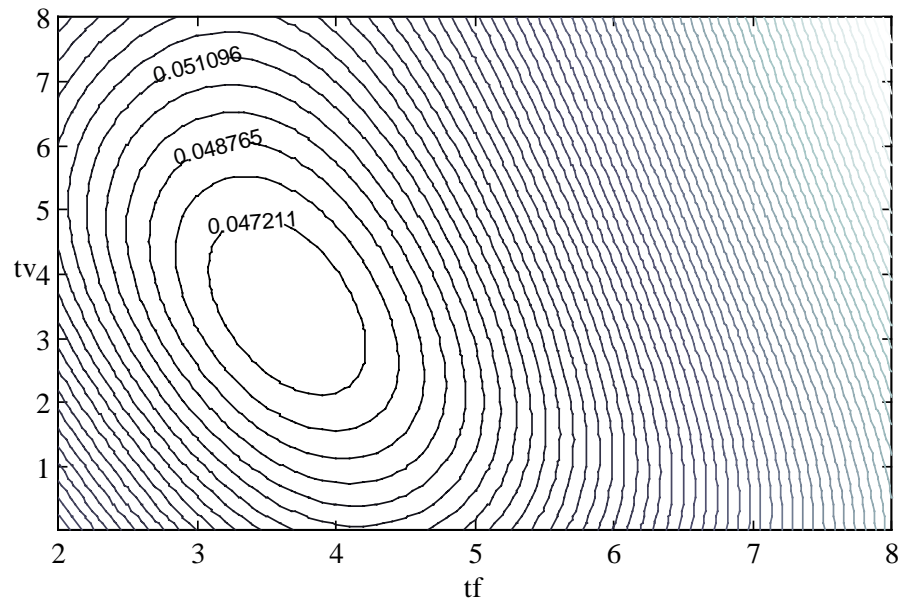


Figure 4.2 Contour plot for the RMS function for NACA 4415 high frequency.

It is of great importance to see how parameters vary depending on what cases that are chosen for the “tuning”. I.e. how much better will the correlation between measurements and simulations be if parameters are “tuned” for the specific case - one airfoil and one time series of airfoil motion - in comparison to if parameters for an average airfoil and a general case is used.

In figure 4.18, 4.20, 4.22, 4.24 and 4.26 the optimized values of  $Tf$  and  $Tv$  are seen for the specific cases as well as some general cases. In figure 4.19 below the RMS values for NACA 4415 calculated with optimized  $Tf$  and  $Tv$  values for the specific case on one hand and some general cases on the other hand. One can use the optimized  $Tf$  and  $Tv$  values of the general cases of all nine Ohio State University case without the RMS value differing that much from the RMS value with  $Tf$  and  $Tv$  values optimized for the specific case, see figures 4.19, 4.21 and 4.23.

Optimization are carried out with  $Tf$ ,  $Tv$  and  $acd$  as design variables,  $Tp=0.8$ ,  $lfmeth=4$  and  $\eta=0.1$

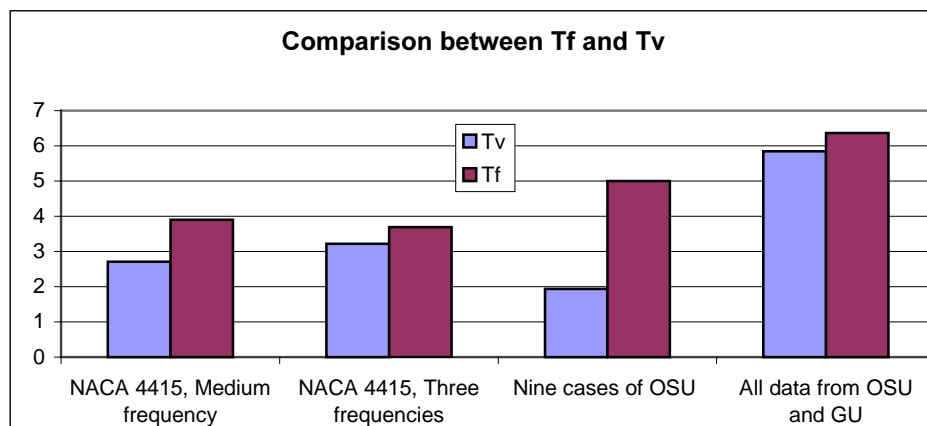


Fig 4.18 Optimized  $T_f$  and  $T_v$  for some cases.

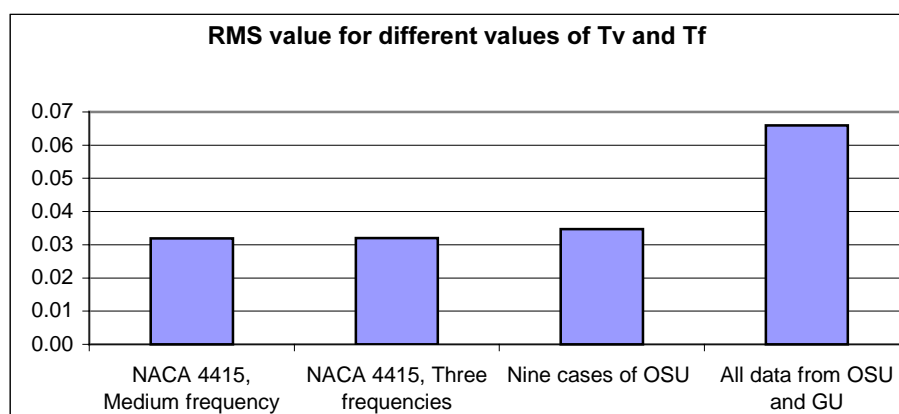


Fig 4.19 RMS values for NACA 4415 medium frequency. Calculations based on  $T_f$  and  $T_v$  values found from optimization for:

1. NACA 4415, medium frequency.
2. NACA 4415, all three frequencies.
3. All Nine OSU-cases
4. All cases from OSU and GU.

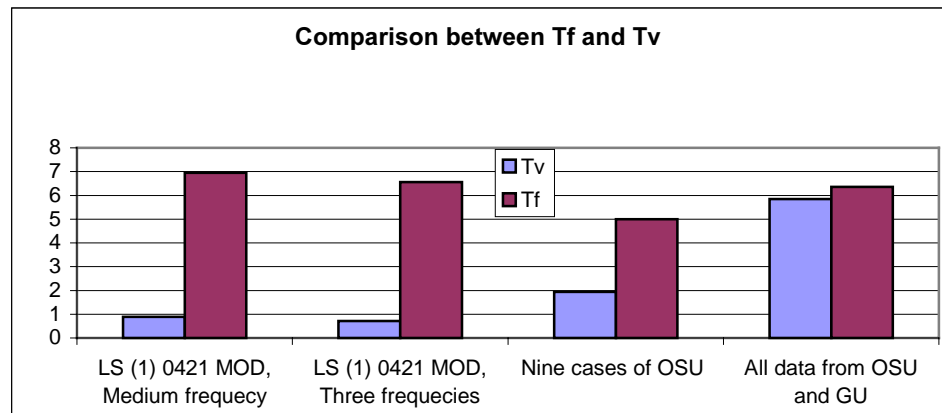


Fig 4.20 Optimized  $T_f$  and  $T_v$  for some cases.

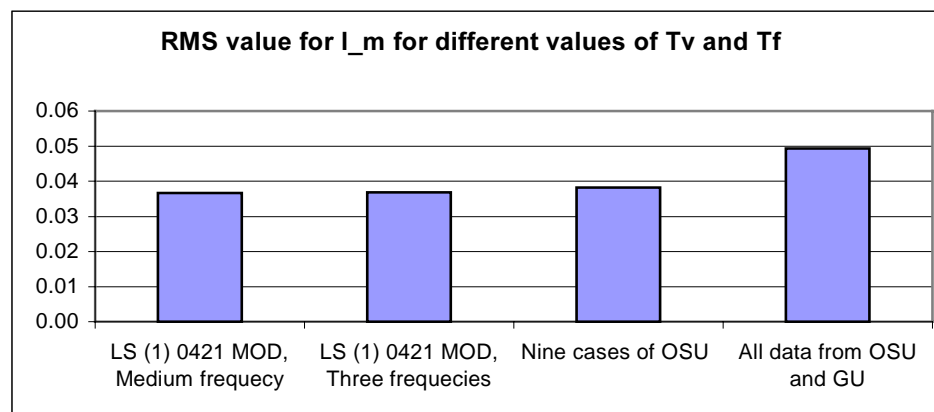


Fig 4.21 RMS values for LS(1) 0421 MOD Medium frequency. Calculations based on  $T_f$  and  $T_v$  values found from optimization for:

1. LS(1) 0421 MOD, medium frequency.
2. LS(1) 0421 MOD, all three frequencies.
3. All Nine OSU-cases
4. All cases from OSU and GU.

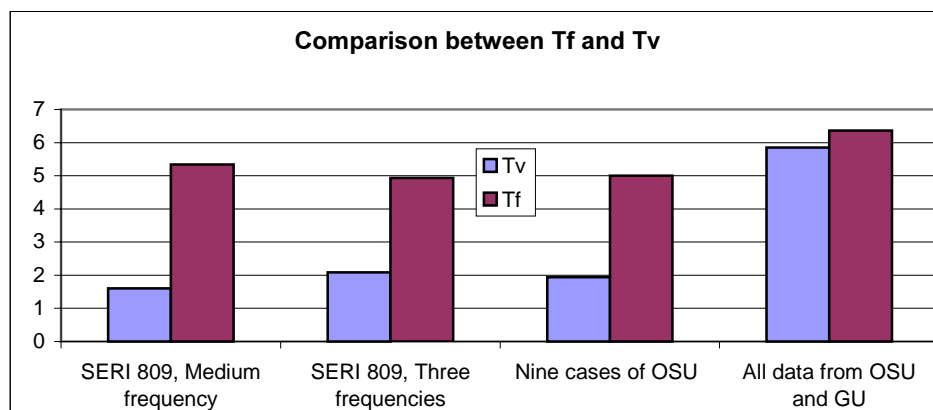


Fig 4.22 Optimized  $T_f$  and  $T_v$  for some cases.

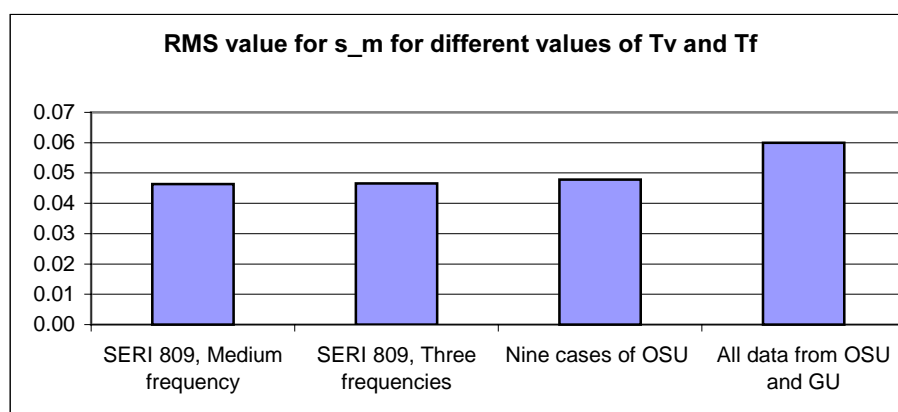


Fig 4.23 RMS values for SERI 809 medium frequency. Calculations based on  $T_f$  and  $T_v$  values found from optimization for:

1. SERI 809, medium frequency.
2. SERI 809 all three frequencies.
3. All Nine OSU-cases
4. All cases from OSU and GU.

For the Glasgow University cases the use of semi-empirical parameters optimized for the general cases, in the calculation of the RMS value for the specific cases does not give much raise to the RMS value. This is only true as long as the general cases have the same mean- $\alpha$  as the specific case, see figure 4.25 and 4.27.

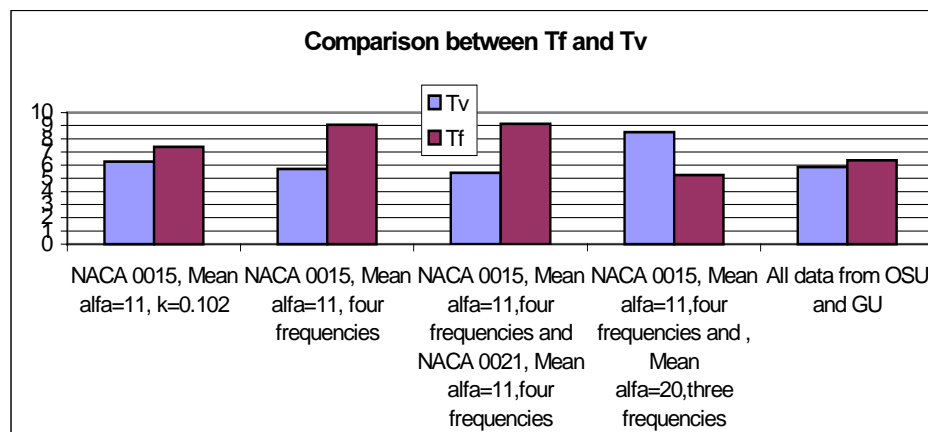


Fig 4.24 Optimized  $T_f$  and  $T_v$ .

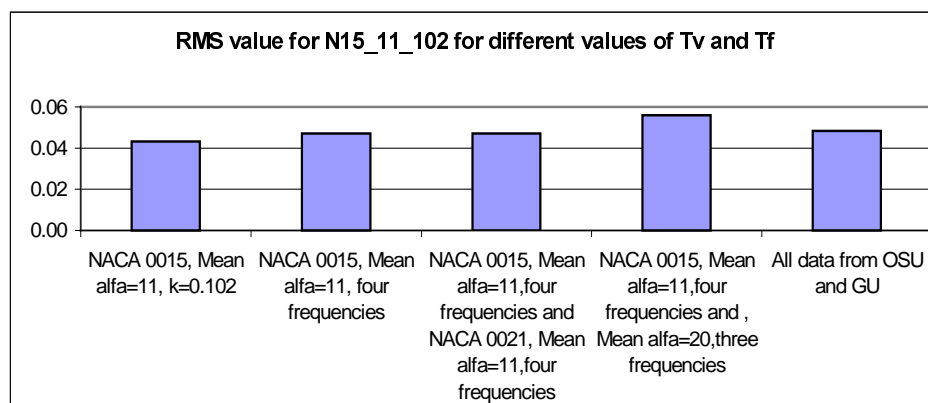
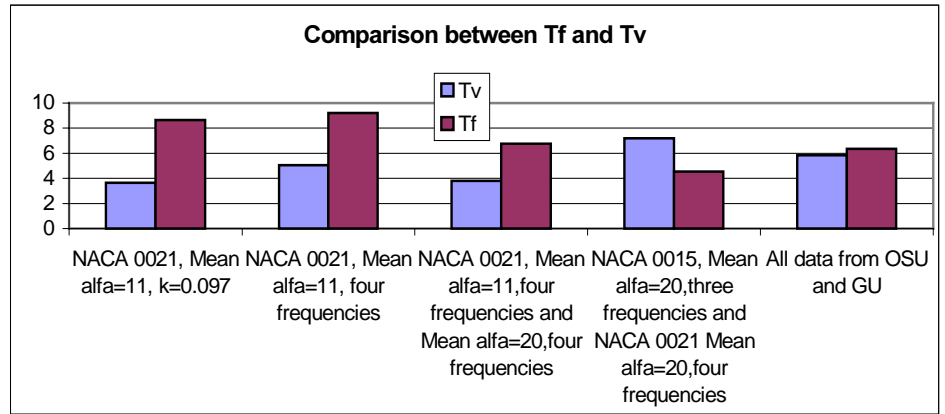
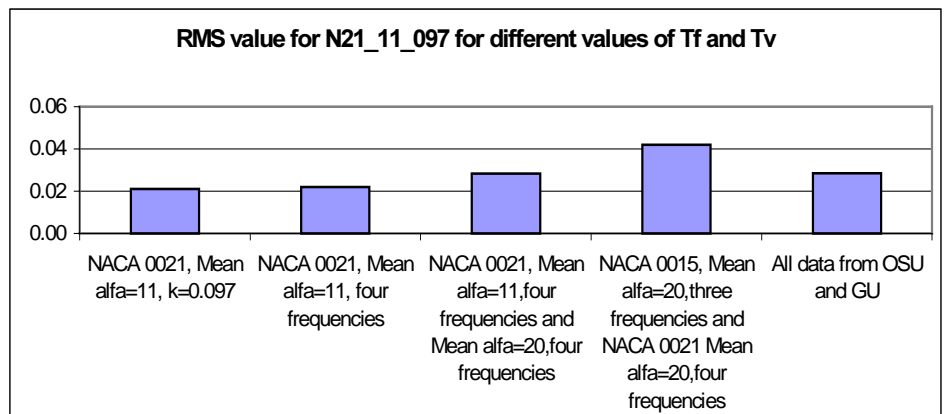


Fig 4.25 RMS values for NACA 0015, Mean  $\alpha=11$ ,  $k=0.102$  calculated using  $T_f$  and  $T_v$  values optimized for different cases.

Fig 4.26 Optimized  $T_f$  and  $T_v$ .Fig 4.27 RMS values for NACA 0021, Mean  $\alpha=11$ ,  $k=0.097$  calculated using  $T_f$  and  $T_v$  values optimized for different cases.

## 4.6 $T_f$ as a function of the separation point

Optimization was also made with a version of the dynamic stall model where  $T_f$  is a function of the separation point  $f$ .  $T_f$  varies linearly between breakpoints. Different values of  $T_f$  at the breakpoints are used for increasing and decreasing angle of attack. In one version (Lfmeth=6) the different values are used depending on the sign of  $\Delta\alpha$ . In another version (Lfmeth=5) different values are used depending on if  $f$  is larger or smaller than  $f_{static}$ , with  $f > f_{static}$  more or less representing increasing

angle of attack. Lfmeth=4 is the version used in optimizations shown earlier with constant Tf.

Four values of Tf at  $f=0$ ,  $f=0.33$ ,  $f=0.66$  and  $f=1$  were used for both increasing and decreasing angle of attack.

An improvement in the RMS function, deviation of observed data from predictions based on the model, could be obtained for each case, see figures 4.28 –4.30

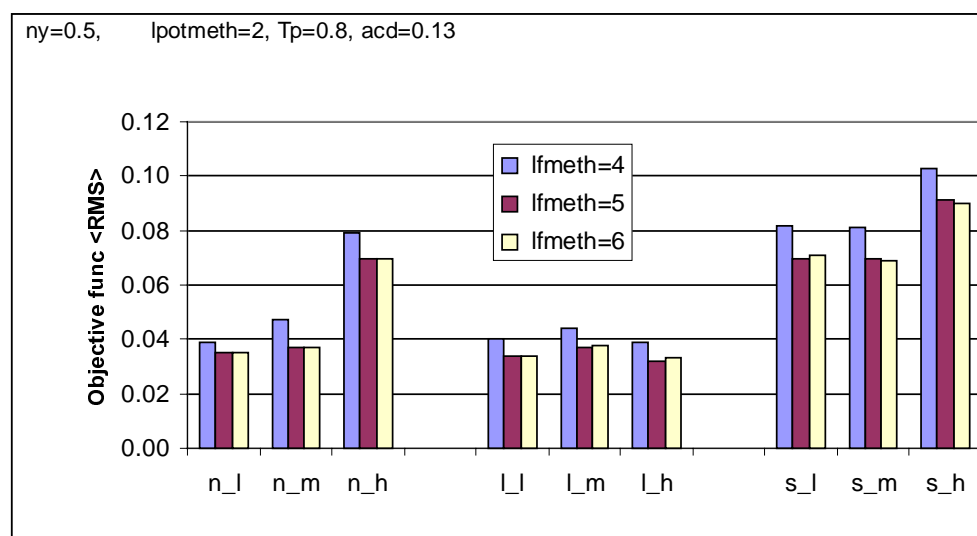


Fig 4.28 RMS values for different cases, calculated with different methods.

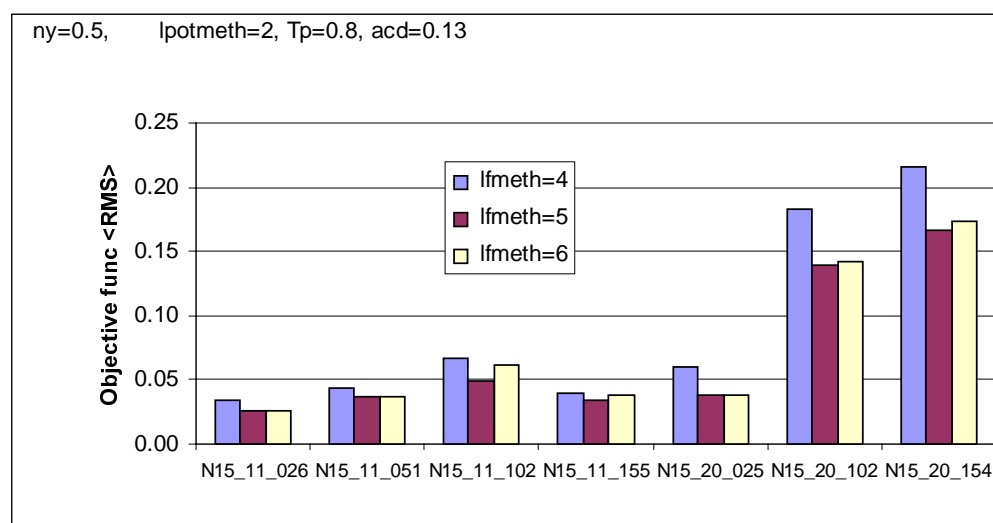


Fig 4.29 RMS values for different cases, calculated with different methods.



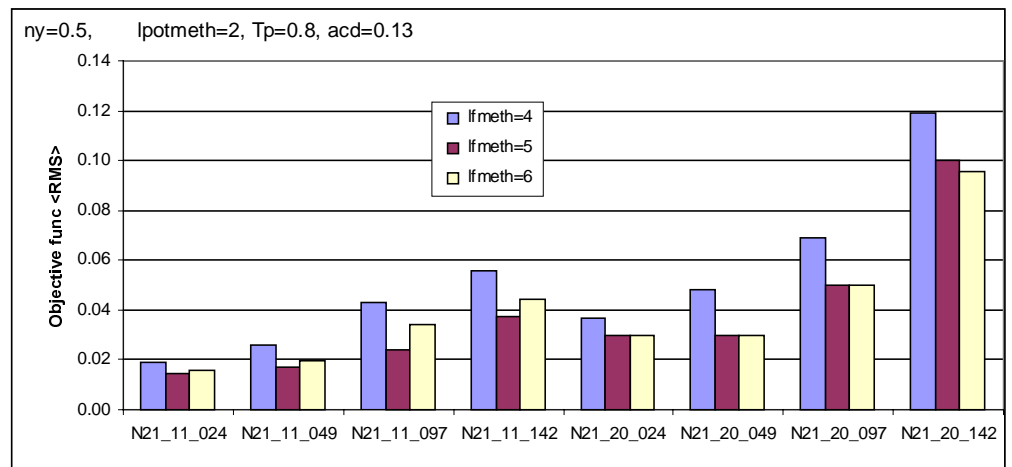


Fig 4.30 RMS values for different cases, calculated with different methods.

However, since no “pattern” in the  $Tf(f)$  variation could be seen no  $Tf(f)$  variation that could be used to represent a good standard variation for a “general airfoil” could be chosen, see figures 4.31-4.33.

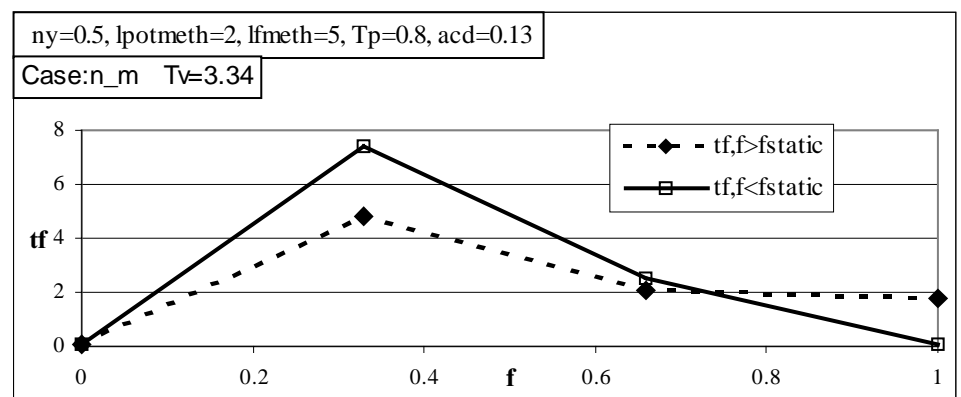


Fig 4.31 Optimized  $Tv$  and  $Tf(f)$  for NACA 4415 medium frequency.

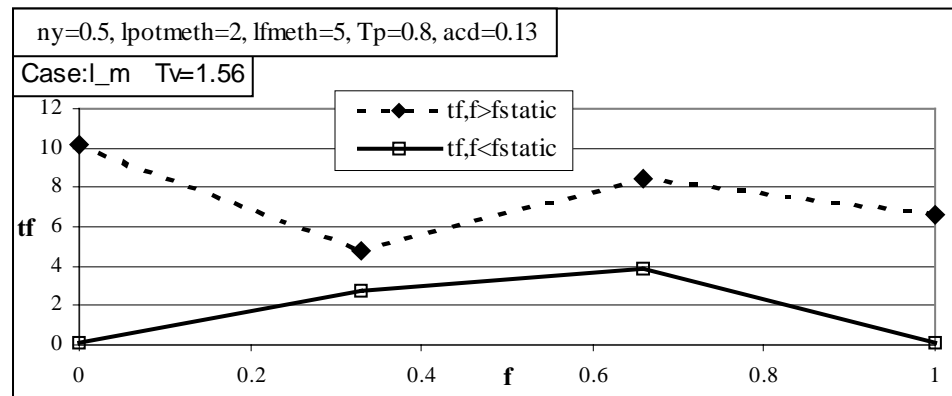
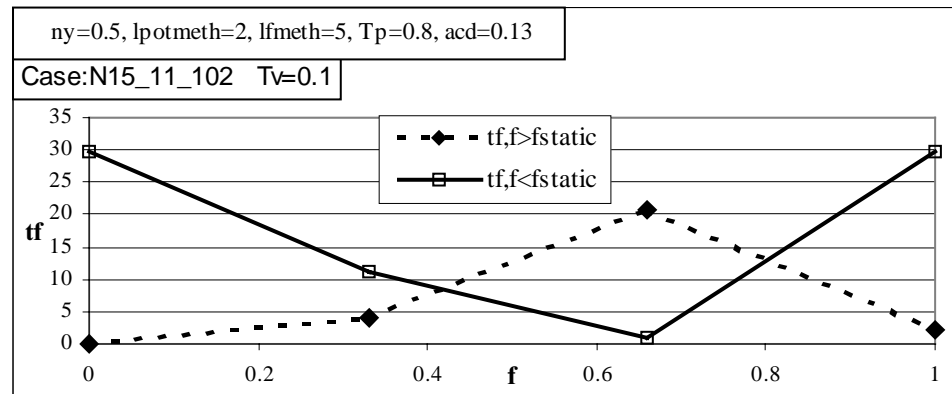


Fig 4.32 Optimized Tv and Tf(f) for LS(1) 0421 MOD medium frequency.

Fig 4.33 Optimized Tv and Tf(f) for NACA 0015 mean  $\alpha=11$ ,  $k=0.102$ .

In figure 4.34 it can be seen that the agreement is good with lfmeth=5 except from a deviation for decreasing angle of attack below  $18^\circ$ . The maximum lift coefficient is badly predicted with lfmeth=4 opposite to the simulation with lfmeth=5.

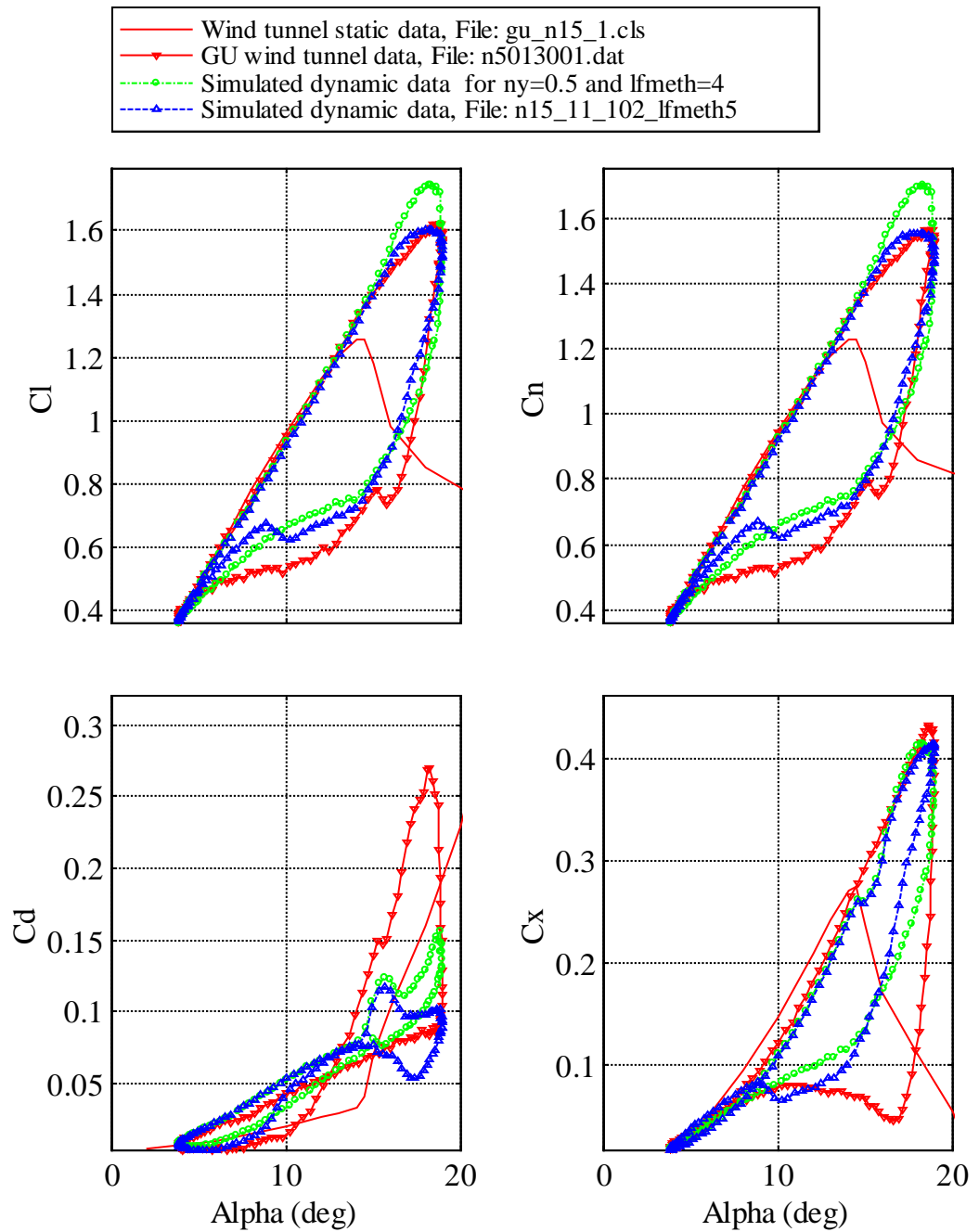


Fig 4.34 Comparison of wind tunnel test data and simulations with  $lfmeth=4$  and  $lfmeth=5$ . Optimized  $T_v=0.1$ . Corresponding values for  $T_f(f)$  can be seen in figure 4.33.



## 5 Conclusions

Numerical optimization was used to find appropriate semi-empirical parameters in the Beddoes dynamic stall model. The optimization is based on minimizing the deviation between results from wind tunnel tests and CFD calculations and results from model simulation.

The optimization tool used is a modified MMA, Method of Moving Asymptotes, package.

In general the comparisons between the aerodynamic force coefficients predicted by the FFA-Beddoes method, using optimized semi-empirical parameters, and measured values are very good. Even though the dynamic stall model is not capable of representing measured dynamic data for high mean- $\alpha$ , large amplitude, deep dynamic stall cases, where a marked vortex shedding process with multiple vortices are present. These are experiments with NACA 0015 and NACA 0021 at mean- $\alpha=20^\circ$  from the University of Glasgow.

The optimization resulted in a large span of the values for the optimized semi-empirical parameters,  $0.0001 \leq T_v \leq 9.45$  and  $1.44 \leq T_f \leq 17.56$ . The optimization for the large amplitude cases of the University of Glasgow with mean- $\alpha=11^\circ$  resulted in larger tuning parameter,  $T_v$  and  $T_f$ , values than for the small amplitude oscillation cases of Risoe. Using  $T_v=2$ ,  $T_f=5$  and  $acd=0.08$  in the model one can get a reasonably good agreement, between measured and simulated data, for a large number of cases, particularly OSU cases.

By letting  $T_f$  be a function of  $f$  an improvement in the RMS function, deviation of observed data from predictions based on the model, could be obtained for each case. However, no “pattern” in the  $T_f(f)$  variation could be seen. Therefore no  $T_f(f)$  variation that could be used for a “general airfoil” could be chosen.

Possible errors in the experiments can have a large impact on the optimized values of the semi-empirical parameters  $T_f$  and  $T_v$ .

Since the set of optimized parameters differ for the plunging and pitching case of CFD calculations, it would be valuable to investigate if this is a general remark or not.



## Acknowledgements

The author would like to acknowledge his supervisor Anders Björck, FFA, for his great support and guidance. Also an acknowledgement to rest of the staff at the Wind Energy Department, FFA, Jan-Åke Dahlberg, Göran Ronsten, Sven-Erik Thor and Rickhard Holm for making the time at FFA very amusing and instructive.

Finally a special thanks to Krister Svanberg, Department of Mathematics, Royal Institute of Technology in Stockholm for being very helpful with my questions concerning the optimization package.





## Referenser

- [1] Lawrence W. Carr. "Progress in Analysis and Prediction of Dynamic Stall." J. Aircraft Vol. 25, NO. 1 pp. 7-8 April 1987
- [2] Robinson, M.C. Galbraith, R.A.M. et.al. "Unsteady Aerodynamics of Wind Turbines", Paper AIAA-95-0526, Reno, USA, January 1995
- [3] Leishman, J.G. Beddoes, T.S. "A Generalized Model for Airfoil Unsteady Aerodynamic Behavior and Dynamic stall Using the Indicial Method" Preceding from 42<sup>nd</sup> Annual Forum of the American Helicopter Society, Washington D.C. June 1986
- [4] Björck, A. "The FFA Dynamic Stall Model. The Beddoes-Leishman Dynamic Stall Model Modified for Lead-lag Oscillations". Conference preceding from IEA 10<sup>th</sup> Symposium on Aerodynamics of Wind Turbines, Edingburgh, G.B, December 1996
- [5] Rasmussen, F. Petersen, J.T. and Madsen, H.A. "Dynamic Stall and Aerodynamic Damping", Paper AIAA-98-0024, Reno, USA, January 1998
- [6] Hoffmann, M. J. et.al. "Unsteady Aerodynamics of Wind turbine Airfoil", Conference preceding from American Wind Energy Association Wind Power 94 conference, Minneapolis, Minnesota, May 9-13, 1994

- [7]

Galbraith, R.A.M.  
et.al.

“Summary of Pressure Data for Thirteen Airfoils on the University of Glasgow’s airfoil Database”, Glasgow University Report 9221, Glasgow, June 1992
- [8]

Fuglesang, P.  
Antoniou, I., Bak, C.  
and Madsen, H.A.

“Wind tunnel Test of the Risoe-1 Airfoil”, Risoe-R999(EN), Risoe, Denmark, May 1998
- [9]

Svanberg, Krister.

“The Method of Moving Asymptotes- A new Method for Structural Optimization”, International Journal for Numerical Methods in Engineering, vol. 24, pp359-373, 1987

# Appendix 1      Manual for the optimization program

## FFA-DYNCLOPT MANUAL

- Write the input values into the input files.  
The input values must be in the following order:
  - If interactive optimization is desired, then 1, if not 0.
  - *Maximum number of iterations.*
  - *Convergence tolerance.*
  - Parameters specifying choice of method in the model.  
*lcncl lpotmeth lfmeth lvormeth lcddyn ldut*
  - Choice of objective function and  $\eta$ .  
Objective function =1:

$$f = \sum_{i=1}^k \eta [(C_{l,sim}(t_i) - C_{l,exp}(t_i))^2]$$

Objective function =2:

$$f = \sum_{i=1}^k \eta [(C_{n,sim}(t_i) - C_{n,exp}(t_i))^2] + \sum_{i=1}^k (1 - \eta) [(C_{t,sim}(t_i) - C_{t,exp}(t_i))^2]$$

*Objective function                       $\eta$*

- Coefficients needed by the model.  
*a1          a2          b1          b2*
- Parameters in the model.  
*Tp Fufac a<sub>cd</sub>*  
*Tvl Tvs                      (not used when lvormeth=2)*
- *Number of design variables*
- Choice of design variables  
design\_var\_opt=1 ==> Tv Tf  
design\_var\_opt=2 ==> Tv Tf acd  
design\_var\_opt=3 ==> Tv Tf1i Tf2i Tf3i Tf4i Tf1d Tf2d Tf3d Tf4d  
design\_var\_opt=4 ==> Tv Tf1i Tf2i Tf3i Tf4i Tf1d Tf2d Tf3d Tf4d  
.....bp1i bp2i bp1d bp2d

design\_var\_opt=5 ==> Tv Tf1i Tf2i Tf3i Tf4i Tf1d Tf2d Tf3d Tf4d  
.....acd

(Design\_var\_opt 3-5 is only valid if lfmeth= 5 or 6)

design\_var\_opt=6 ==> Tv Tf acd Tp

*Design\_var\_opt*

- Initial guess for the design variables.  
*designvariable\_1 designvariable\_2.....designvariable\_N*
- Minimum values for the design variables.  
*min\_1 min\_2.....min\_N*
- Maximum values for the design variables.  
*max\_1 max\_2.....max\_N*
- *dx* in the calculations of the differentials.
- Coefficient used in the model.  
*cnlpos cnlneg* (not used when lvormeth=2)
- *Pivot point.*
- Parameters specifying choice of method in the model.  
*alfa\_input\_meth dtau\_max*
- *Number of static data files*
- Number of measured data files per static data file.  
*x1(for the first static data file)*  
*x2(for the second static data file)*  
.  
.  
*xN(for the N<sup>th</sup> static data file)*
- *Name and location for the first static data file.*  
*Name and location for the first measured data file*  
*P1 P2 chord length of the airfoil .*  
(P1-P2 are the measured data points the optimization is made for)  
*Name and location for the second measured data file*  
*P1 P2 chord length of the airfoil.*  
.  
.  
*Name and location for the N<sup>th</sup> measured data file*  
*P1 P2 chord length of the airfoil.*

- *Same as above for the rest of the static data files.*
- Comments  
*Commentline1*  
*Commentline2*  
*Commentline3*
- Names and locations of the output files (without three letter extension).  
*File1 ==>*  
File1.utd, contains some input values and the optimization result.  
File1.txt, contains the comment lines.  
File1.log, log file over design variables and corresponding RMS value for each iteration.

*DataResultfile1 ==>* DataResultfile1.utd, containing resulting dynamic load coefficient, among other things, simulated, using optimized parameters, for the first case.

*DataResultfile2 ==>* DataResultfile2.utd, containing resulting dynamic load coefficient, among other things, simulated, using optimized parameters, for the second case.

.

*DataResultfileN ==>* DataResultfileN.utd, containing resulting dynamic load coefficient, among other things, simulated, using optimized parameters, for the N<sup>th</sup> case.

- ❑ Write the names and locations of the input files into the input specification file
- ❑ Run the optimization program.

## An example of the input file:

```
#           Selection of interactive optimization
# interactive optimization = yes ==> interactive=1
# interactive optimization = no ==> interactive=0
# interactive
#           0
#-----
#           Convergence criteria - If batch mode is chosen
# Maximum number of iterations
#           30
# Convergence tolerance
```

```
1.d-5
#-----
# lcncl   lpotmeth   lfmeth   lvormeth   lcddyn   ldut
#      2       2       4       2       1       0
#-----
# Objective function            $\eta$ 
#      2               0.5
#-----
# a1,      a2,      b1,      b2
#   0.3    0.7    0.14    0.53
#-----
# First row: tp          fufac          acd
#             0.8        0.5          0.13
#-----
# vortex parameters (1 row)
#   tvl          tvs
#     8           0
#-----
# number of design variables
#     3
#-----
# Choose design variables
#design_var_opt=1 ==> tv tf
#design_var_opt=2 ==> tv tf acd
#design_var_opt=3 ==> tv tf1i tf2i tf3i tf4i tf1d tf2d tf3d tf4d
#design_var_opt=5 ==> tv tf1i tf2i tf3i tf4i tf1d tf2d tf3d tf4d acd
#design_var_opt=6 ==> tv tf acd tp
#           2
#-----
#   tvinitial   tfinitial   acdinitial
#       8d0       8d0       0.13d0
#-----
#   tvmin       tfmin       acdmin
#    1d-4       1d-4       1d-4
#-----
#   tvmax       tfmax       acdmax
#    30d0       30d0       2d0
#-----
#   dx_val
#    0.0001
#-----
# cnlpos       cnlneg
#    1.7       -2
```

```
#-----
# pivot
#   0.25
#-----
# alfa_input_meth   dtau_max
#       2           0.2
#-----
# number of .cls files
#   2
#-----
#number of .dat files per .cls file
#   1
#   2
#-----
# File name with "sep-data" .cls files
#-----
#   p1  till      p2      chord  (c_in)
#-----
#File name with experimental data .dat files
#-----
s:\mtm\prof_data\gu_prof\gu_n15_1.cls
#-----
s:\mtm\prof_data\gu_prof\n5012641.dat
#   129      256                      .55
#-----
s:\mtm\prof_data\gu_prof\gu_n21_1.cls
#-----
s:\mtm\prof_data\gu_prof\n7012641.dat
#   129      256                      .55
s:\mtm\prof_data\gu_prof\n7012781.dat
#   129      256                      .55
#-----
# Comment lines (3 rows)
Comment1
Comment2
Comment3
#-----
# Location and name of outputfiles without three letter extension
s:\mtm\dyncl_in_ut\dyncl_utdatafiler\output_file
s:\mtm\dyncl_in_ut\dyncl_utdatafiler\dyn_datafile1
s:\mtm\dyncl_in_ut\dyncl_utdatafiler\dyn_datafile2
s:\mtm\dyncl_in_ut\dyncl_utdatafiler\dyn_datafile3
```

## An example of the Result file:

\*\*\*FFA-Beddoes Dynamic Stall Model INPUT VARIABLES AND THE RESULTS\*\*\*

=====

Indatafile used :

=====

s:\mtm\dyncl\_in\_ut\dyncl\_indatafiler\in3var\_12\_ny05

lcnc lpotmeth lfmeth lvormeth lcddyn ldut

2 2 4 2 1 0

Objective function= 2

Pivot= 0.25

Ny= 0.50

Dat file used :

=====

s:\mtm\prof\_data\gu\_prof\n5012641.dat

s:\mtm\prof\_data\gu\_prof\n7012641.dat

s:\mtm\prof\_data\gu\_prof\n7012781.dat

Number of iterations: 10

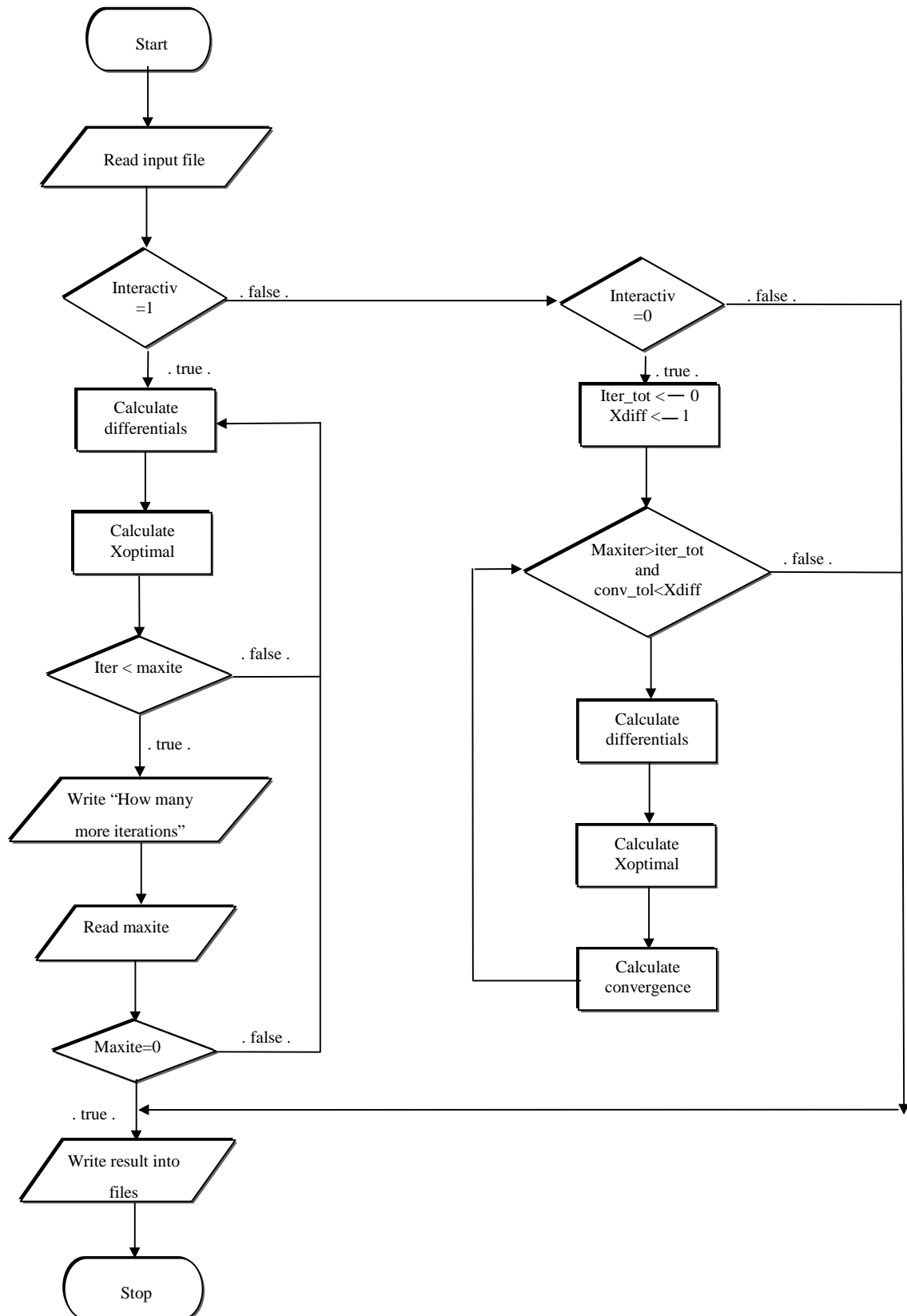
Optimized values of design parameters:

j	xval(j)
=====	=====
1	0.0001
2	7.9121
3	0.0589

RMS value = 0.0561



## Appendix 2 Flow chart for the optimization program





## Appendix 3 Data for optimization cases

Cases for Optimization				
Airfoil	Mean alfa	Alfa amplitude	Reduced Frequency	Abbreviation
<b>Ohio State University wind tunnel test</b>				
NACA 4415	14.2	10.8	0.023	n_l
	14.2	10.8	0.046	n_m
	14.2	10.8	0.069	n_h
	13.2	10.5	0.022	l_l
	13.2	10.5	0.045	l_m
	13.2	10.5	0.066	l_h
	12.9	10.6	0.02	s_l
	12.9	10.6	0.041	s_m
	12.9	10.6	0.061	s_h
<b>Glasgow University wind tunnel test</b>				
NACA 0015	11.3	8.0	0.026	N15_11_026
	11.3	7.9	0.051	N15_11_051
	11.4	7.6	0.102	N15_11_102
	11.1	7.0	0.155	N15_11_155
	19.8	7.6	0.025	N15_20_025
	19.8	7.4	0.102	N15_20_102
	19.6	6.8	0.154	N15_20_154
NACA 0021	10.9	7.9	0.024	N21_11_024
	10.9	7.8	0.049	N21_11_049
	10.0	7.8	0.097	N21_11_097
	11.0	7.7	0.142	N21_11_142
	19.9	7.9	0.024	N21_20_024
	19.9	7.9	0.049	N21_20_049
	19.8	7.9	0.097	N21_20_097
	19.9	7.8	0.142	N21_20_142
<b>Risoe wind tunnel data</b>				
Risoe-1	11.8	1.6	0.11	dclm02dcdm007
<b>Risoe CFD (Ellipsys unsteady calc with k-w SST )</b>				
Risoe-1	11.8	1.6	0.11	CFD Plunging
	11.8	1.6	0.11	CFD Pitching



## Appendix 4 Classification of Cases and Optimization Results

OSU NACA 4415, three frequencies → Group(1)

OSU LS(1) 0421 MOD, three frequencies → Group(2)

OSU SERI 809, three frequencies → Group(3)

GU NACA 0015, mean- $\alpha = 11^\circ$ , four frequencies → Group(4)

GU NACA 0021, mean- $\alpha = 11^\circ$ , four frequencies → Group(5)

GU NACA 0015, mean- $\alpha = 20^\circ$ , three frequencies → Group(6)

GU NACA 0021, mean- $\alpha = 20^\circ$ , four frequencies → Group(7)

Table A4.1 Optimization result for  $T_p=0.8$  and  $\eta=0.1$ .

Optimization result				
Case	Tv	Tf	acd	RMS
n_l	3.11	3.52	0.0001	0.0268
n_m	2.71	3.9	0.0094	0.0319
n_h	3.56	3.57	0.035	0.0535
l_l	0.0023	6.12	0.0001	0.031
l_m	0.89	6.95	0.0001	0.037
l_h	0.77	6.45	0.017	0.03
s_l	0.0001	10.92	0.076	0.0483
s_m	1.6	5.34	0.11	0.0463
s_h	3.33	4.03	0.16	0.063
N15_11_026	2.13	12.26	0.056	0.025
N15_11_051	6.35	8.21	0.139	0.029
N15_11_102	6.26	7.39	0.165	0.043
N15_11_155	6.65	14.56	0.156	0.023
N15_20_025	2.42	9.59	0.27	0.048
N15_20_102	9.15	3.55	0.43	0.12
N15_20_154	9.29	4.1	0.2	0.17
N21_11_024	1	13.57	0.0001	0.0098
N21_11_049	2.23	10.9	0.032	0.016
N21_11_097	3.65	8.66	0.14	0.02
N21_11_142	7.05	9.98	0.17	0.027
N21_20_024	0.92	9.42	0.0001	0.032
N21_20_049	1.56	5.8	0.075	0.032
N21_20_097	3.4	6.37	0.09	0.055
N21_20_142	5.61	5.48	0.095	0.097
Group (1)	3.22	3.69	0.023	0.04
Group (2)	0.72	6.56	0.0083	0.033
Group (3)	2.09	4.93	0.11	0.057
Group (4)	5.71	9.07	0.14	0.036
Group (5)	5.04	9.2	0.14	0.022
Group (6)	9.24	3.56	0.41	0.13
Group (7)	3.85	5.93	0.088	0.062
Group (1+2+3)	1.94	5	0.037	0.046
Group (1+2+3+4+5+6+7)	5.85	6.36	0.13	0.074
Group (4+5)	5.42	9.13	0.14	0.03
Group (4+6)	8.51	5.23	0.17	0.094
Group (5+7)	3.79	6.75	0.097	0.05
Group (6+7)	7.19	4.54	0.18	0.098
dclm02dcdm007	1.21	4.18	0.0001	0.0064
Risplunge	0.0001	8.66	0.0001	0.0037
Rispitch	1.37	1.44	0.1	0.0032

Table A4.2 Optimization result for  $T_p=0.8$  and  $\eta=0.5$ .

Optimization Result				
Case	Tv	Tf	acd	RMS
n_l	3.14	3.52	0.014	0.039
n_m	2.7	3.93	0.019	0.046
n_h	4.62	2.64	0.15	0.079
l_l	0.45	5.4	0.0001	0.04
l_m	3.91	3.46	0.15	0.044
l_h	2.02	4.96	0.071	0.039
s_l	0.0001	9.28	0.17	0.082
s_m	0.0001	7.03	0.011	0.08
s_h	0.137	6.43	0.0001	0.1
N15_11_026	3.28	11.1	0.088	0.034
N15_11_051	2.93	11.22	0.07	0.044
N15_11_102	3.13	10.43	0.11	0.067
N15_11_155	4.94	17.56	0.15	0.039
N15_20_025	0.0001	12.27	0.12	0.06
N15_20_102	4.91	8.82	0.0001	0.18
N15_20_154	8.82	10.7	0.0001	0.21
N21_11_024	0.081	14.72	0.0001	0.015
N21_11_049	0.4	13.11	0.008	0.021
N21_11_097	2.6	10	0.11	0.043
N21_11_142	6.36	11.29	0.13	0.056
N21_20_024	1.36	8.91	0.027	0.036
N21_20_049	1.23	6.18	0.044	0.047
N21_20_097	2.63	7.4	0.035	0.067
N21_20_142	3.38	9.64	0.0001	0.1154
Group (1)	3.73	3.23	0.085	0.058
Group (2)	2.35	4.66	0.081	0.042
Group (3)	0.0001	6.78	0.0001	0.089
Group (4)	2.47	11.97	0.099	0.052
Group (5)	3.6	10.95	0.1	0.041
Group (6)	6.3	9.1	0.0001	0.17
Group (7)	2.39	7.74	0.0093	0.079
Group (1+2+3)	1.66	5.28	0.034	0.068
Group (1+2+3+4+5+6+7)	2.02	9.81	0.0001	0.11
Group (4+5)	3.16	11.48	0.1	0.047
Group (4+6)	5.9	9.65	0.027	0.12
Group (5+7)	2.31	8.71	0.033	0.067
Group (6+7)	4.15	8.68	0.0001	0.13
dclm02dcdm007	1.74	3.47	0.0001	0.0108
Risplunge	0.0001	8.23	0.013	0.0072
Rispitch	1.28	1.55	0.12	0.0057

Table A4.3 Optimization result for  $\eta=0.1$ .

Optimization Result					
	Tv	Tf	acd	Tp	RMS
n_l	3.18	4.15	0.006	0.0001	0.027
n_m	2.9	4.35	0.032	0.0001	0.032
n_h	3.78	4	0.064	0.0001	0.0526
l_l	0.0001	6.89	0.0001	0.0001	0.031
l_m	1.04	7.51	0.01	0.0001	0.0356
l_h	1.08	6.85	0.037	0.0001	0.0287
s_l	0.0001	11.34	0.086	0.0001	0.0477
s_m	2.2	5.46	0.15	0.0048	0.046
s_h	3.21	4.3	0.15	0.52	0.0632
N15_11_026	2.43	12.77	0.068	0.0001	0.0248
N15_11_051	6.01	7.44	0.11	1.99	0.0284
N15_11_102	7.55	5.27	0.1	3.44	0.0407
N15_11_155	6.71	14.33	0.15	0.88	0.0226
N15_20_025	0.59	8.85	0.15	4	0.0439
N15_20_102	8.48	2.55	0.15	4	0.1074
N15_20_154	9.26	2.57	0.12	4	0.1415
N21_11_024	1.04	13.76	0.0001	0.558	0.0098
N21_11_049	3.29	10.94	0.055	0.0001	0.0153
N21_11_097	0.0001	6.35	0.079	3.48	0.018
N21_11_142	8.23	7.04	0.11	3.18	0.0244
N21_20_024	0.96	10.04	0.005	0.0001	0.0317
N21_20_049	1.03	3.88	0.017	3.97	0.0304
N21_20_097	2.74	5.13	0.0454	2.72	0.0528
N21_20_142	5.57	5.39	0.09	0.91	0.0965
Group (1)	3.41	4.14	0.047	0.0001	0.0387
Group (2)	0.98	7.03	0.025	0.0001	0.0319
Group (3)	2.34	5.06	0.13	0.37	0.0568
Group (4)	5.07	7.44	0.093	2.84	0.035
Group (5)	4.55	7.83	0.1	2.35	0.021
Group (6)	8.8	2.58	0.14	4	0.1099
Group (7)	3.45	5.28	0.06	1.79	0.0611
Group (1+2+3)	2.29	5.33	0.06	0.0001	0.0454
Group (1+2+3+4+5+6+7)	5.18	4.45	0.07	4	0.0713
Group (4+5)	4.88	7.61	0.097	2.64	0.029
Group (4+6)	8.6	3.2	0.11	4	0.0833
Group (5+7)	2.99	5.72	0.059	2.36	0.0488
Group (6+7)	7.078	2.71	0.11	4	0.0889
dclm02dcdm007	1.38	4.94	0.0001	0.0001	0.0054
Risplunge	0.0001	9.53	0.001	0.0001	0.0031
Rispitch	1.38	2.24	0.11	0.0001	0.0029



Table A4.4 Optimization result for  $\eta=0.5$ .

Optimization Result					
	Tv	Tf	acd	Tp	RMS
n_l	3.04	4.35	0.012	0.0001	0.0386
n_m	2.69	4.03	0.018	0.68	0.0462
n_h	4.46	3.42	0.15	0.0001	0.078
l_l	0.41	3.25	0.0001	3.25	0.0387
l_m	3.74	4.34	0.15	0.0001	0.0434
l_h	2.08	5.3	0.078	0.36	0.0387
s_l	0.0001	10.04	0.15	0.008	0.0806
s_m	0.0001	7.58	0.005	0.0001	0.0773
s_h	0.425	6.8	0.0001	0.0008	0.0987
N15_11_026	3.37	10.55	0.055	1.3	0.0334
N15_11_051	3.46	11.46	0.08	0.16	0.0432
N15_11_102	0.0001	7.91	0.06	3.64	0.0561
N15_11_155	0.0001	12.0951	0.1147	3.4654	0.0327
N15_20_025	0.0001	9.9	0.12	4	0.0514
N15_20_102	4.59	7.34	0.0001	2.49	0.1754
N15_20_154	9.45	7.14	0.0001	4	0.1977
N21_11_024	0.28	15.26	0.0001	0.09	0.0151
N21_11_049	1	13.49	0.017	0.0001	0.0193
N21_11_097	0.0001	6.6	0.063	4	0.0292
N21_11_142	5.84	7.32	0.084	4	0.039
N21_20_024	1.39	9.56	0.03	0.0001	0.0361
N21_20_049	0.95	3.97	0.028	4	0.042
N21_20_097	1.63	5.94	0.002	3.26	0.0613
N21_20_142	3.08	9.5	0.0001	1.11	0.1153
Group (1)	3.46	4.11	0.069	0.0001	0.0572
Group (2)	2.37	5.31	0.09	0.064	0.0417
Group (3)	0.146	7.25	0.0001	0.0001	0.0877
Group (4)	0.0001	10.22	0.065	3.06	0.048
Group (5)	1.35	8.35	0.064	3.59	0.0352
Group (6)	6.64	6.3	0.019	3.47	0.1647
Group (7)	1.43	6.76	0.0001	2.69	0.0766
Group (1+2+3)	1.78	5.84	0.038	0.0001	0.067
Group (1+2+3+4+5+6+7)	0.56	8.77	0.0001	3.04	0.108
Group (4+5)	0.1	9.62	0.06	3.3	0.0424
Group (4+6)	5.72	7.38	0.03	3.27	0.1167
Group (5+7)	0.97	6.78	0.0001	3.65	0.0618
Group (6+7)	3.19	7.66	0.0001	2.6	0.1313
dclm02dcdm007	1.82	4.31	0.0001	0.0001	0.0088
Risplunge	0.0001	9.04	0.016	0.0001	0.006
Rispitch	1.11	2.56	0.09	0.0001	0.0047





Issuing organization  The Aeronautical Research Institute of Sweden (FFA) P.O. Box 11021 S-161 11 BROMMA, Sweden	Document no.		
	FFA TN 1999-37		
	Date June 1999	Security Unclassified	
Sponsoring agency Swedish National Energy Administration FFA internal research funds	Reg. No.	No. of pages 83	
	Project no. Vu 0313 Ve 0184 Ve 0199	Order/Contract STEM P11556-1	
Title Optimization of Semi-Empirical Parameters in the FFA-Beddoes Dynamic Stall Model			
Author  Murat Mert			
Checked by  Anders Björck Wind Energy Section, FFA		Approved by  Sven-Erik Thor Head Wind Energy Section, FFA	
Abstract <p>Unsteady aerodynamic effects, like dynamic stall, must be considered in calculation of dynamic forces for wind turbines. Models incorporated in aero-elastic programs are of semi-empirical nature. Resulting aerodynamic forces therefore depend on values used for the semi-empirical parameters. In this report a study of finding appropriate parameters to use with the FFA- Beddoes-Leishman dynamic stall model is discussed. Minimization of the deviation between results from 2D wind tunnel tests and simulation with the model is used to find optimum values for the parameters.</p> <p>The optimization program MMA, Method of Moving Asymptotes is used to optimize parameters in the model for nonlinear aerodynamics.</p> <p>The optimization program MMA has been modified to work for problems with a quadratic object function without constraints.</p> <p>The resulting optimum parameters show a large variation from case to case. Using these different sets of optimum parameters in the calculation of blade vibrations give rise to quite different predictions of aerodynamic damping.</p>			
Key words Dynamic stall, Optimization, Wind energy, Semi-empirical parameters, Unsteady aerodynamics			
Distribution	STEM	VKK-råd	FFA
Copy No.	1-7	8-17	18-60